5-2014

# Effects of Heregulin on Muscle: A Biochemical and Histological Analysis

Nicole Justine Moss
*Dominican University of California*

https://doi.org/10.33015/dominican.edu/2014.bio.04

**Survey: Let us know how this paper benefits you.**

**Effects of Heregulin on Muscle: A Biochemical and Histological Analysis**

A thesis submitted to the faculty of
Dominican University of California
& BioMarin Pharmaceutical Inc.
in partial fulfillment of the requirements
for the degree

Master of Science
in
Biology

By
Nicole Moss
San Rafael, California
May, 2014

## CERTIFICATION OF APPROVAL

I certify that I have read Effects on Heregulin on Muscle: A Biochemical and Histological Analysis by Nicole Moss, and I approved this thesis to be submitted in partial fulfillment of the requirements for the degree: Master of Sciences in Biology at Dominican University of California and BioMarin Pharmaceutical Inc.

_____

**Paul Fitzpatrick, PhD**

Graduate Research Advisor,
Director of Protein Sciences
Research, BioMarin Pharmaceutical
Inc.  Novato, CA

_____

**Sean Bell, PhD**

Thesis Second Reader, Senior
Scientist of Protein Sciences
Research, BioMarin Pharmaceutical
Inc.  Novato, CA

_____

**Mary B. Sevigny, PhD**

Graduate Program Coordinator,
Assistant Professor Dominican
University, San Rafael, CA

**Abstract**:

Duchenne Muscular Dystrophy, the most common inherited X-linked genetic disease affecting 1 in 5000 boys, results from a dysfunctional dystrophin protein encoded by the *DMD* gene. Dystrophin interacts with protein complexes linking the extracellular matrix to the cytoskeleton of muscle fibers. Without dystrophin functioning properly, sarcolemmal membrane stabilization is compromised during the mechanical rigors involved with muscle contraction leading to progressive muscular dystrophy. Heregulin/neuregulin-1 (HRG), a member of the epidermal growth factor family has been shown to induce neuromuscular junction (NMJ) gene expression *in vitro* and improve skeletal muscle function in dystrophic mice. However, it is unclear if the HRG effects were due to proliferation, cell survival, differentiation, or stimulation of NMJ formation to improve excitation-contractile coupling. To identify a mechanism of action, HRG effects were investigated through *in vitro* and *in vivo* experiments: characterization of downstream signaling, observation of the effects on acetylcholine receptor clustering *in vitro*, and observation of NMJ morphology *in vivo*. In this study we show through Western blots and electrochemiluminesence assays that AKT and ERK were activated by HRG, but downstream effects were not clear. HRG decreased laminin-induced AChR clusters in a dose dependent manner *in vitro,* resulting in the possible reorganization of AChRs. *In vivo*, HRG was found to partially restore NMJ formation and increase axonal and muscle integration in the NMJ. This study provides evidence that a mechanism of action for the positive effects of HRG on the dystrophic phenotype in *mdx* mice are due

to a reorganization of AChRs and an improvement in NMJ formation, potentially improving excitation contraction coupling.

**Acknowledgements:**

# Table of Contents

# Figures

**Abbreviations:**

**α-btx**: α-bungarotoxin

**ACh:** Acetylcholine

**AChR:** Acetylcholine Receptor

**BMD:** Becker's Muscular Dystrophy

**DMD:** Duchenne Muscular Dystrophy

**ECL:** Electrochemiluminescence

**ECLA:** Electrochemiluminescence Assay

**EGF:** Epidermal growth factor

**GSK-3β**: Glycogen synthase kinase 3β

**HRG:** Heregulin-β1

**IHC:** Immunohistochemistry

**JNK:** c-Jun N-terminal kinase

***mdx*:** Duchenne Muscular Dystrophy mouse model

**NF:** neurofilament

**NMJ:** Neuromuscular Junction

**nNOS:** Neuronal nitric oxide synthase

**NRG:** Neuregulin

**PBS**: Phosphate-buffered saline

**RTK:** Receptor Tyrosine Kinase

**SDS-PAGE**: Sodium dodecyl sulfate-polyacrylamide gel electrophoresis

**TA:** Tibialis anterior

**TBS:** Tris-buffered saline

**Veh**: Vehicle

**WT:** Wild Type

**Introduction:**

**Duchenne muscular dystrophy**

Duchenne Muscular Dystrophy (DMD) was first described in 1861 by Edward Meryon followed by documentation in more detail by Guillaume-Benjamin-Amand Duchenne in 1868 (Emery & Emery, 1993). Duchenne reported a boy with calf muscle hypertrophy and evidence of a muscle disease though a histological examination of his muscle, which is known today as a muscle biopsy (Emery & Emery, 1993; Parent, 2005). The genetics of DMD were characterized in the 1980's leading to the discovery that patients with DMD have an absence or dysfunction of the protein dystrophin in 1987 (Davies et al., 1983; Hoffman, Brown, & Kunkel, 1987).

DMD, the most common muscular dystrophy and X-linked genetic disorder affecting 1 in 5000 boys, belongs in a class of non-congenital early childhood-onset muscular dystrophies, with Becker muscular dystrophy being a milder version of Duchenne seen later in childhood to adulthood (Mendell & Lloyd-Puryear, 2013; Mercuri & Muntoni, 2013).  Usually by the age of 2-3, but sometimes as late as 5 or 6 years, patients with DMD will show symptoms of muscle weakness such as walking on toes, calf hypertrophy with a slow or awkward gait, exhibit fatigue, have trouble getting up from a sitting or lying position, and have frequent falls (Cyrulnik, Fee, De Vivo, Goldstein, & Hinton, 2007; Khurana & Davies, 2003; Sharma, Mynhier, & Miller, 1995). As a result of the progressive muscle weakness associated with the disease, children are usually late to walk and will use the Gowers' maneuver to rise up off the floor, which is a common warning sign for parents and physicians (Bushby et al., 2010). DMD burdens

patients while performing daily tasks such as playing with other children and climbing stairs due to progressive muscle weakness (Khurana & Davies, 2003). Eventually, muscle weakness is so severe that children around age 10 become permanently wheelchair-bound (Voisin & de la Porte, 2004). About 30% of DMD patients have mental retardation and associated comorbidities such as autism and ADHD (Cyrulnik et al., 2008; Pane et al., 2012). Death usually occurs from cardiac or pulmonary failure in a patient's second or third decades of life (Finder et al., 2004).

DMD pathology is characterized by a repetitive cycle of muscle damage followed by muscle regeneration and tissue inflammation resulting in progressive muscle loss and the replacement of healthy tissue with fibro-fatty tissue (Figure 1 and 3) (Archer, Vargas, & Anderson, 2006; Khurana & Davies, 2003; Voisin & de la Porte, 2004). DMD patients experience a progressive loss of muscle mass and function in lower leg muscle (Cros, Harnden, Pellissier, & Serratrice, 1989). Hypertrophy is one of many dramatic phenotypes seen in early childhood and is characterized in DMD patients by the gain of mass in calf muscles due to the replacement of muscle with fibro-fatty tissue (Khurana & Davies, 2003; Verma, Anziska, & Cracco, 2010). Although symptoms can be treated to some extent and research has progressed over the past few decades, there is no cure. The most common treatment option is glucocorticoids, which can prolong ambulation but have consequential side effects such as obesity, short stature, cataracts and withdrawal (Manzur, Kuntzer, Pike, & Swan, 2004; Schara, Mortier, & Mortier, 2001). Glucocorticoids only slow the progression of the disease while slightly enhancing strength by reducing inflammation through immunosuppression (Finder et al., 2004;

Joshi & Rajeshwari, 2009; Verma et al., 2010). Overall, DMD is an X-linked genetic

disorder resulting in progressive muscle degeneration, cardiac dysfunction, respiratory

deficiency, and early mortality.
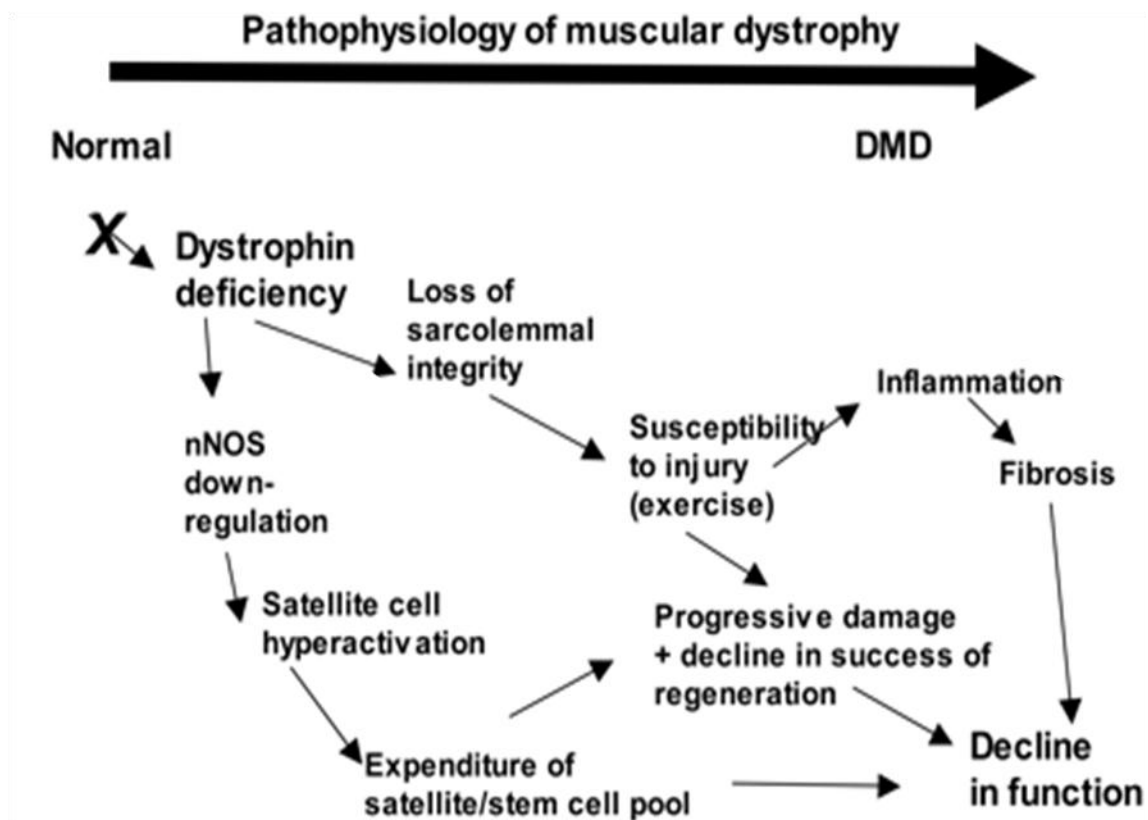


**Figure 1: Pathophysiology of muscular dystrophy**
Adapted from Archer et al., 2006.

**Dystrophin**

Dystrophin, a 427-kDa protein, is encoded by the largest gene in the human

genome (*DMD*) at 2.5Mb of genomic sequence that can code for 79 exons (J. M. Tinsley,

Blake, Zuellig, & Davies, 1994; Wells, 2008). Dystrophin has an important structural role

linking the dystrophin-associated glycoprotein complex at its C-terminus to F-actin at its

N-terminus and maintaining sarcolemmal integrity. (Ferlini, Neri, & Gualandi, 2013;

Nowak & Davies, 2004). An example of the dystrophin-associated glycoprotein complex and associated proteins is shown below in Figure 2. A key feature of dystrophin that sets it apart from its homolog, utrophin, is the interaction with neuronal nitric oxide synthase (nNOS) at its C-terminus. In the absence of functional dystrophin, nNOS is located in the cytosol rather than near the sarcolemma and is unable to properly function during a muscle contraction resulting in insufficient blood supply, or ischemia, which can cause cell necrosis in skeletal and cardiac muscle cells (Heydemann & McNally, 2004; Sander et al., 2000). The dystrophin protein is also essential for neuromuscular junction (NMJ) architecture and folding of post-synaptic membranes, which contain acetylcholine receptors (AChR) (Shiao et al., 2004).

DMD results from mutations in the dystrophin gene (*DMD*) located on the X chromosome (Xp21); mutations in the *DMD* gene are responsible for the missing or defective dystrophin protein (Davies et al., 1983; Ferlini et al., 2013; Saito et al., 1993; Tayeb, 2010). Large deletions in the *DMD* gene occur in 60% of DMD patients (Voisin & de la Porte, 2004). Point mutations, which usually introduce a premature stop codon, small deletions and duplications represent the other *DMD* mutations (Voisin & de la Porte, 2004). It is estimated that mothers who are carriers of *DMD* mutations are responsible for approximately two thirds of patients while the other patients are from spontaneous germline mutations in the *DMD* gene (Roberts, 1995).
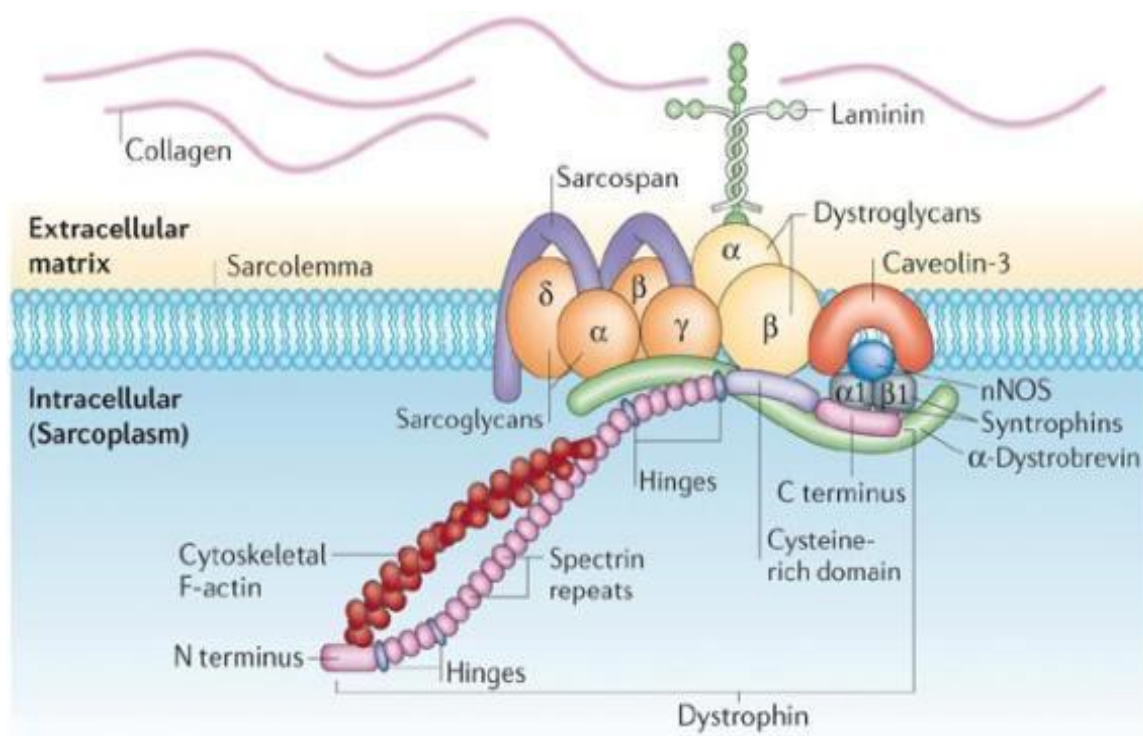
**Figure 2: Dystrophin-associated glycoprotein complex**
Dystrophin provides a crucial mechanical link between the extracellular matrix and intracellular cytoskeleton. (Davies & Nowak, 2006)

**DMD pathology**

When dystrophin is absent or truncated, a DMD patient's muscles deteriorate and weaken (Wells, 2008). Muscle contraction can cause the weakened sarcolemma to become increasingly prone to rupture, leading to increased membrane permeability to $Ca^{2+}$ (B J Petrof, 1993; Mallouk, Jacquemond, & Allard, 2000; Pato, Davis, Doughty, Bryant, & Gruenstein, 1983; Turner, Westwood, Regen, & Steinhardt, 1988). The elevated $Ca^{2+}$ levels are speculated to contribute to an increased activation of $Ca^{2+}$-dependent proteases that could affect cell function/viability and early deterioration of essential proteins in the dystrophin-associated glycoprotein complex (Imbert, Cognard,

Duport, Guillou, & Raymond, 1995; Ohlendiec, 2002). In addition, altered calcium levels affect $Ca^{2+}$-gated $K^+$-channels, membrane potential and activation potential for muscle contraction (Turner et al., 1988). Compromised sarcolemma initiates muscle repair, as the plasma membrane is a vital barrier and essential for cell survival (Han, Rader, Levy, Bansal, & Campbell, 2011; Head, 1993; Mallouk et al., 2000). During muscle injury mitochondria migrate to the area of injury and block off damaged tissue, while muscle stem cells (satellite cells) proliferate at the site, fuse to form new tubes, fuse with damaged muscle fibers and restore muscle fiber integrity (Wallace & McNally, 2009). In patients with DMD, damaged muscle attempts to compensate for tissue injury with help from satellite cell proliferation, myoblast differentiation and repair; yet, endeavors at repair are met with partial success and inflammation from macrophage infiltration and fibrosis are often a result of tissue damage (Nowak & Davies, 2004). Due to the excessive regeneration of skeletal muscle in patients with DMD, satellite stem cell populations quickly become depleted preventing muscle repair and results in dystrophic muscle (Jejurikar & Kuzon, 2003). An example of DMD muscle pathology is shown in Figure 3.
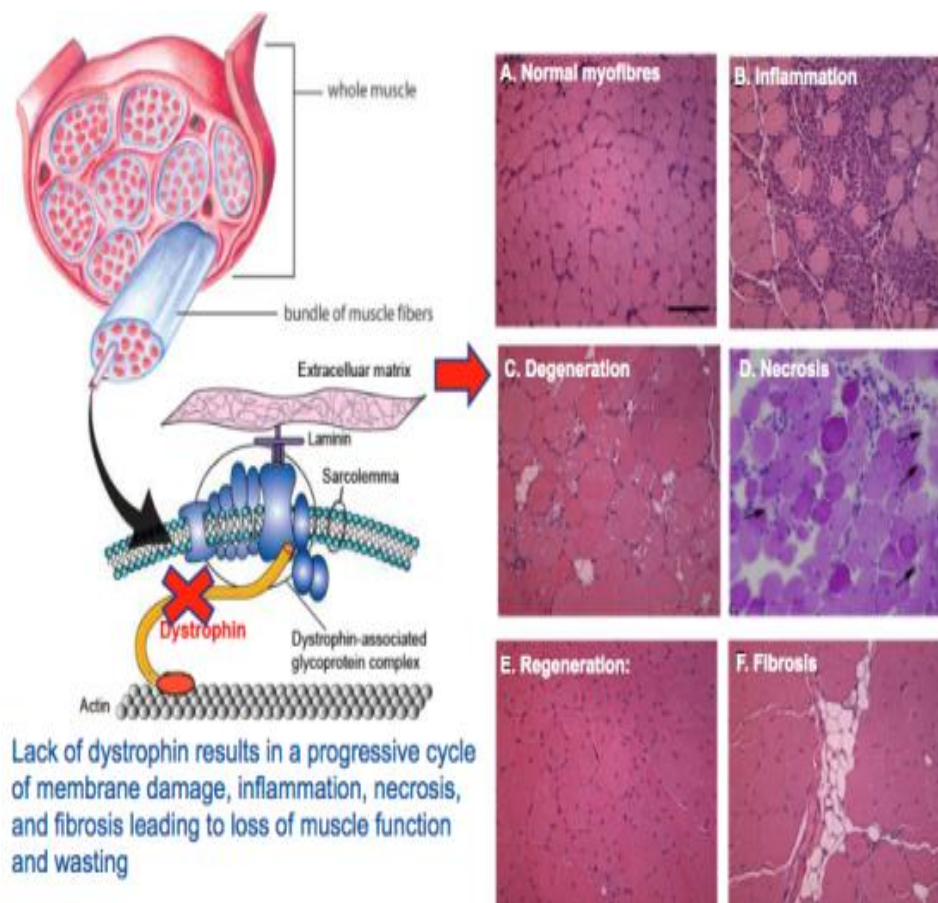
**Figure 3: DMD muscle pathology**
H&E staining of normal (A) and DMD (B-F) muscle tissue showing the consequences due to the absence of dystrophin resulting in: inflammation (B), degeneration (C), necrosis (D), regeneration (E), and fibrosis (F) (BioMarin internal figure, courtesy of Sean Bell).

Dystrophin-deficiency is also responsible for NMJ fragmentation on regenerating muscle fibers (Kong & Anderson, 1999). Since dystrophin is required for AChR organization, the absence of dystrophin contributes to the reduction and distribution of AChR clustering over time (Personius & Sawyer, 2005). Nerve-dependent mechanisms are also responsible for the spatial organization of AChRs (Marques, Pertille, Carvalho, & Santo Neto, 2007) .

DMD is lethal. DMD patients are caught in a vicious cycle of progressive muscle damage and tissue repair. Muscle stem cells can only compensate for so long due to extensive depletion before necrosis occurs initiating a fatty, fibrous-like, tissue replacement. Regardless of improvements in medical technology and prolongation of survival of DMD patients within in the past decades, DMD invariably results in death usually by cardiac or respiratory failure (Passamano et al., 2012).

**_mdx_, a mouse DMD model**

To better understand DMD disease pathology, animal models of dystrophin-deficiency are used, such as the _mdx_ mouse (Bulfield, Siller, Wight, & Moore, 1984; Ryder-Cook et al., 1988). The _mdx_ mouse carries a premature stop codon at exon 23 preventing the production of a functional dystrophin protein (Im et al., 1996). _Mdx_ mice have a slightly shorter lifespan, reduced cardiac function, and a progressive loss and/or damage to skeletal muscle (Nowak & Davies, 2004). The disease phenotype in _mdx_ mice is much less severe when compared to humans. _Mdx_ mice show less fibrosis, a near normal lifespan and are completely mobile when compared to boys with DMD (Chamberlain, Metzger, Reyes, Townsend, & Faulkner, 2007). It is believed the mild _mdx_ phenotype is due to increased compensatory utrophin expression and higher muscle regeneration capacity in mice (Chamberlain et al., 2007; Pons, Robert, Marini, & Leger, 1994; Weir, Morgan, & Davies, 2004).

As evidence of the effect of the higher regeneration capacity of mice compared to boys, a dystrophin deficient mouse strain with fewer satellite cells or with reduced

proliferative capacity was generated. Dystrophin- and telomerase-deficient mice were generated and shown to have significantly impaired proliferation potential of muscle satellite cells, and a more sever dystrophic phenotype representative of human disease, including much earlier mortality (Mourkioti et al., 2013; Sacco et al., 2010). Unfortunately, due to the lack of the availability of this model and the challenging nature of developing dystrophin- and telomerase-deficient mice, only *mdx* mice were available for this study.

**The therapeutic potential of Heregulin β-1**

HRG, a trophic factor encoded by the Neuregulin-1 gene *(NRG1)*, is one protein of potentially fifteen splice variants (Falls, 2003; Holmes et al., 1992) (Figure 4). During embryogenesis, HRG is necessary and involved in glial growth, cardiac development, and acts as a neuronal cell differentiation factor (Britsch, 2007; Vartanian, Fischbach, & Miller, 1999) . Mice that lack HRG die in utero due to cardiac defects (Barros et al., 2009; Ueda et al., 2005). Although HRG is normally associated with neuronal tissue, HRG is also endogenously expressed in muscle cells and vascular endothelium (Britsch, 2007). However, mice lacking muscle-derived HRG live post partum, which confirms that HRG is not essential for muscle development (Jaworski & Burden, 2006). Not only does HRG have developmental roles, but HRG has positive effects on muscle function and provides protection from cerebral and cardiac ischemic injury in adults (Britsch, 2007; Fang et al., 2010; Zhao et al., 1998).
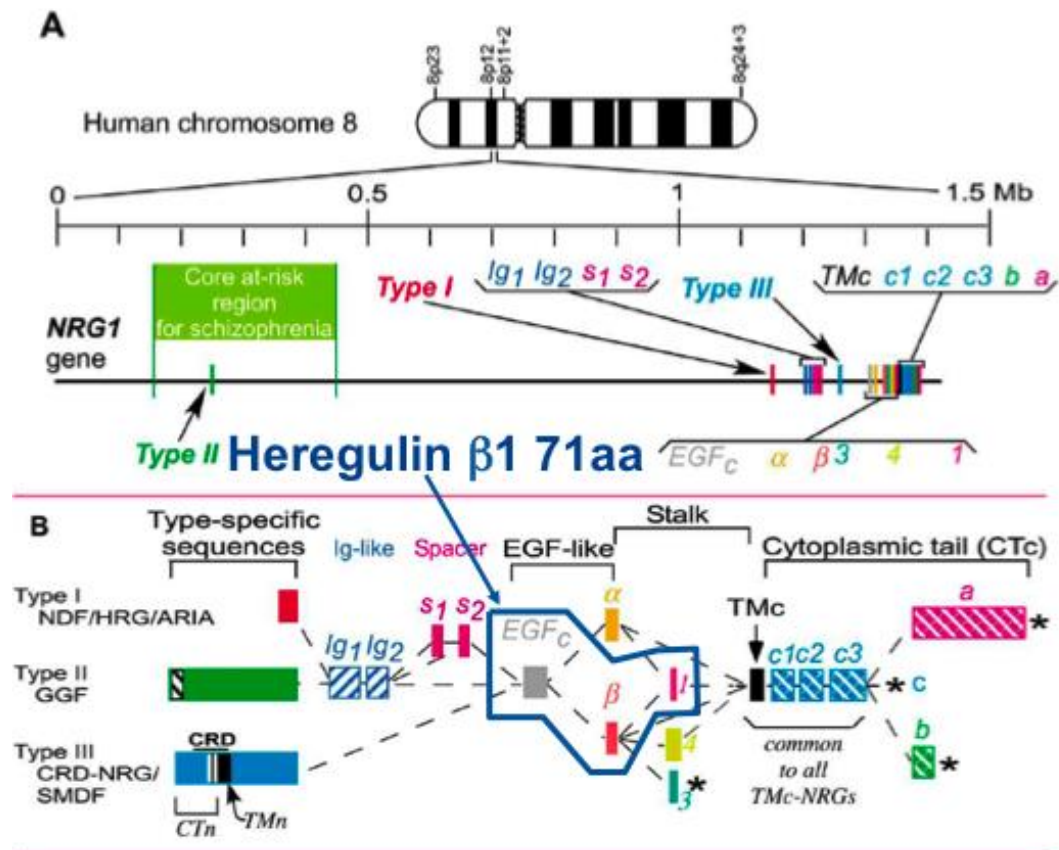
**Figure 4: NRG1 gene and gene products**
The *NRG1* gene and several potential isoforms. A) The location and genomic structure of *NRG1.* B) NRG1 splice varients and resulting protein products. The 71 amino acid fragment of HRG β-1 encoding only the EGF domain used for this study is outlined in blue. (Adapted from Falls, 2003.)

**HRG signaling via ErbB2**

HRG initiates various functions through the activation of the kinase ErbB2 and its downstream signaling (Earp, Calvo, & Sartor, 2003; Plowman et al., 1993). HRG binds to the extracellular domain of ErbB3/ErbB4, which then heterodimerizes with ErbB2 to initiate signaling by phosphorylation of the intracellular C-terminal domain as a result of the heterodimeric receptor tyrosine kinase (RTK) formation between ErbB2/3 (or ErbB2/4) (Negro, Brar, & Lee, 2004; Odiete, Hill, & Sawyer, 2012; Roskoski, 2012). When

ErbB2/3 is activated by HRG, AKT (Protein Kinase B), and ERK 1/2 (Extracellular Receptor Kinase / Mitogen-activated Protein Kinase) can be downstream signaling targets (Falls, 2003; Roskoski, 2012). HRG signaling is not a straight line. HRG-associated signaling pathways and potential cellular effects are shown in Figure 5 (Newbern & Birchmeier, 2010).
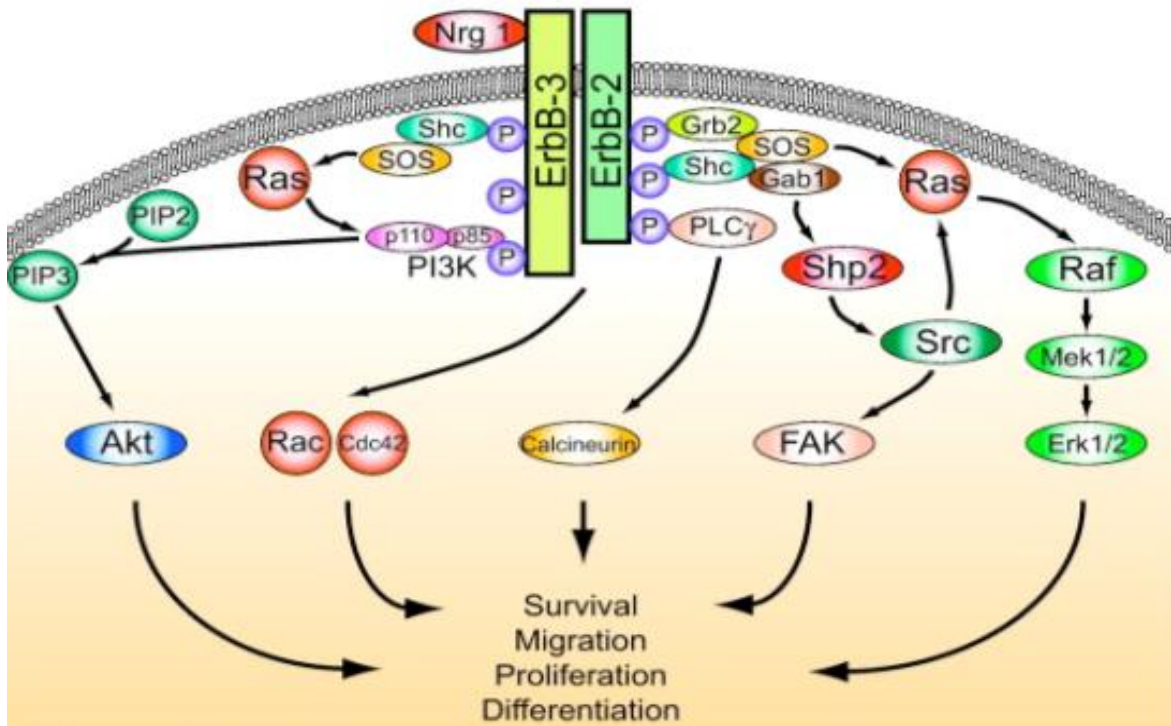


**Figure 5: Heregulin (NRG1) signaling pathways and cellular effects**
(Newbern & Birchmeier, 2010).

**HRG and neuromuscular junctions**

NMJs are important for the transmission of signals from nerves to muscle and require Acetylcholine receptor (AChR) clustering for accurate signaling (Ferraro, Molinari, & Berghella, 2012). One of many neurotransmitters, acetylcholine (ACh), is released from the nerve terminal to communicate instantaneously with a muscle fiber

to orchestrate the appropriate muscle contraction (Fagerlund & Eriksson, 2009; Sudhof, 2004; Vartanian et al., 1999). When ACh is released from the motor neuron, it binds to the AChR at a 2:1 ratio inducing the depolarization of the postsynaptic membrane and stimulates muscle contraction (Fagerlund & Eriksson, 2009).

NMJs have a high degree of plasticity and are constantly remodeled due to muscle contraction, making each NMJ unique (Pratt et al., 2013). Following muscle injury, the axon branches will regenerate to reform synapses (Pratt et al., 2013). NMJs in mdx mice are shown to be particular susceptible to damage and may contribute to dystrophic muscle (Pratt et al., 2013). NMJs are malformed in DMD patients as well as in *mdx* mice and demonstrate a discontinuous bouton formation as shown in Figure 6. In *mdx* mice, axonal branching is increased and bundles of AChRs are dispersed resulting in NMJ fragmentation (Pratt et al., 2013).

In the peripheral nervous system, Schwann cells form a necessary protective myelin sheath that promotes faster nerve impulses and while residing at the NMJ, help to stabilize the interaction with muscle through adherence to the basement membrane (Corfas, Velardez, Ko, Ratner, & Peles, 2004). In a recent publication, HRG signaling response in Schwann cells restored thickness of the myelin sheath and induced hypermyelination of damaged nerves (Stassart et al., 2013). HRG signaling via ErbB2 is known to regulate AchR gene transcription and other proteins in NMJs (Bezakova & Ruegg, 2003; Handschin et al., 2007).
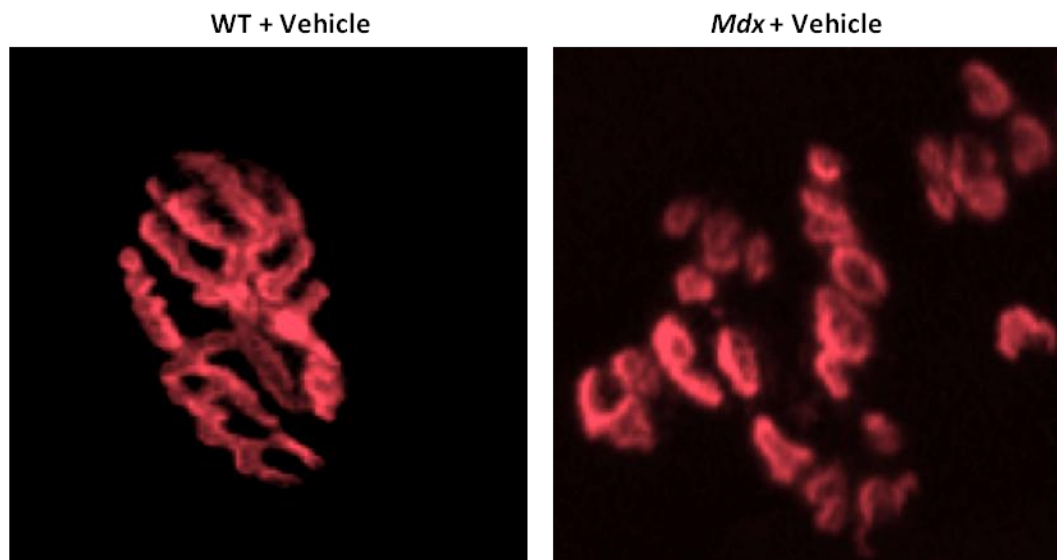
**Figure 6: WT and mdx NMJs**
NMJs were identified by labeling AChRs with α-bungarotoxin-alexa fluor 555 and imaged by confocal microscopy. Wild type (WT) mouse (Left) showing a continuous "pretzel – like" NMJ formation and an *mdx* mouse (Right) showing a discontinuous bouton NMJ formation distributed in islands due to the absence of the dystrophin protein.

HRG may affect NMJ formation though ERK activation. Through *in vitro* experiments, HRG activated ERK in C2C12 myoblasts and myotubes resulted in the up-regulation of NMJ genes which can be beneficial for NMJ formation and possibly translate to the restoration muscle function (Handschin et al., 2007; Tansey, Chu, & Merlie, 1996). HRG effects on NMJ formation may improve the excitation-contraction coupling, an action potential resulting in a contraction, which is defective in DMD patients due to poorly formed NMJs (Schertzer, van der Poel, Shavlakadze, Grounds, & Lynch, 2008). Signaling from the HRG-ERK-NMJ gene up-regulation pathway at the NMJ is shown in Figure 7 (Bezakova & Ruegg, 2003).
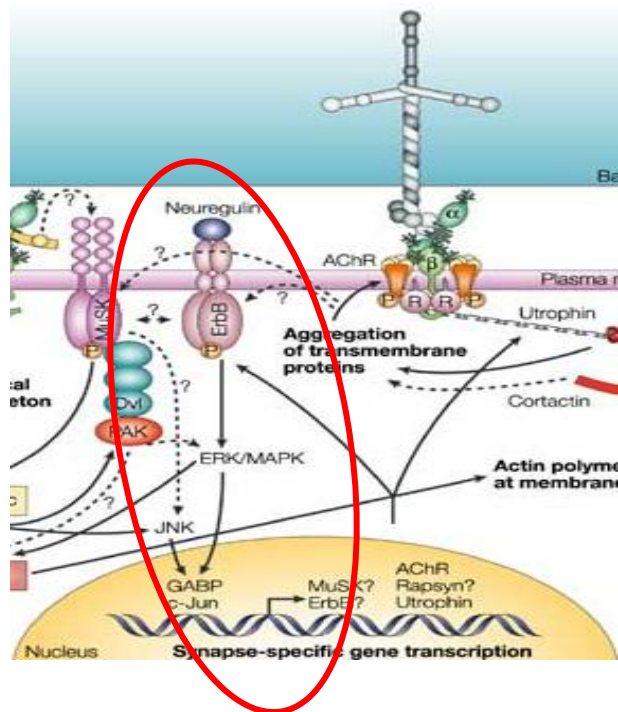
**Figure 7: HRG signaling at the NMJ**
HRG is shown to regulate transcription of AChR and other NMJ genes though its receptor kinase, ErBb2/3 (adapted from Bezakova G & Ruegg M, 2003).

**Heregulin and utrophin**

Heregulin β-1 (HRG) has shown therapeutic qualities in the *mdx* mouse as well as an effect on utrophin levels *in vitro* (Basu et al., 2007; Gramolini et al., 1999; Krag et al., 2004). Utrophin, an autosomal homolog of dystrophin, forms a similar utrophin-associated glycoprotein complex in the neuromuscular junction and has an 80% homology to dystrophin (Marshall & Crosbie-Watson, 2013; Voisin & de la Porte, 2004). Utrophin up-regulation is a popular therapeutic theory for the substitution of dystrophin. Utrophin has been shown to be up-regulated by HRG in C2C12 cells and in *mdx* mice (Basu et al., 2007; Handschin et al., 2007; Krag et al., 2004). It was observed that the transgenic induction of utrophin improved the dystrophic phenotype in *mdx* mice (Nowak & Davies, 2004; J. Tinsley et al., 1998). HRG-treated mice were also shown

to have improved strength, decreased inflammation, and reduced muscle damage; this improvement was postulated to be mediated by an increase in utrophin (Krag et al., 2004).

One of the limitations in the Krag study was the small number of mice studied. The *mdx* mouse phenotype is highly variable. Only five mice were treated and it has been shown by Nagaraju and Wilmann that a minimum of 10 mice are needed to significantly power an *mdx* therapeutic study (Nagaraju & Willmann, 2009). It was proposed by Krag that a two-fold induction of utrophin was sufficient to ameliorate the dystrophic phenotype. Results from experiments performed at BioMarin have shown 2-fold differences in utrophin protein and mRNA levels between individual *mdx* mice; such individual variation raises questions about the significance of such a small change in utrophin levels (S. Bell, personal communication). Although no clear mechanism of action was identified, HRG had beneficial therapeutic effects improving the dystrophic-phenotype (S. Bell, personal communication).

**Hypothesis**

DMD is a progressive muscle wasting disease with no cure. HRG was shown to alleviate the dystrophic phenotype in *mdx* mice. HRG has also been shown to activate ERK in C2C12 myotubes inducing the gene transcription of many NMJ proteins including the dystrophin homolog, utrophin. Although utrophin did not appear to be significantly affected by HRG *in vivo*, ERK involvement in other proteins involved in NMJ function would be of interest. AKT has been shown to be important for muscle health and fiber type switching to promote stronger fibers and has been identified as a downstream

target of HRG signaling. Based on these observations, it is hypothesized that HRG activation of ERK and AKT and the activation of proteins downstream of AKT and ERK might be responsible for NMJ gene induction, improved cell survival, or other effect that ameliorated the dystrophic phenotype observed in HRG-treated *mdx* mice. Specifically, AChR clustering and NMJ formation were of interest as they had previously been identified as downstream targets of HRG and ERK signaling. This thesis evaluated the effects of HRG on muscle biochemically, through cell signaling assays, and histologically, by analysis of AChR clustering *in vitro* and NMJ formation *in vivo,* to elucidate a mechanism of action.

**Materials and Methods:**

**C2C12 cell culture and myotube differentiation**

C2C12 mouse myoblasts were cultured in DMEM (Dulbecco's Modified Eagle Medium) high glucose plus GlutaMAX with 1% Pen/Strep and 10% fetal bovine serum (normal growth medium) (all from Life Technologies) (McMahon et al., 1994). Cells were between 2 and 10 passages before seeding into 6, 12, or 96 well cell culture treated plates (Costar) and maintained at ≤50% confluency. To differentiate myoblasts into myotubes, cells were grown to 80% confluency and switched to DMEM containing 2% horse serum (Invitrogen) for at least 3 days for differentiation and then switched back to normal growth medium.

**Signaling and cell lysis**

A 71 amino acid rhHRG fragment encoding only the EGF domain was obtained from R&D Systems and resuspended in Tris-buffered saline (TBS). Cultured myoblasts or myotubes were serum-starved for up to 4 hours and then treated with phosphate-buffered saline (PBS, vehicle) or HRG up to 1600ng/mL, washed with ice cold PBS, and lysed by the addition of a sufficient amount of RIPA buffer (Sigma) containing phosphatase and protease inhibitors (Pierce) at various time points. Each condition was collected separately and centrifuged. The pellets were discarded and supernatants reserved. All samples were then kept on ice for the duration of the experiment or stored frozen at -80°C for later analysis.

Total protein concentration of cell supernatants was determined by a BCA protein Assay Kit (Pierce). Samples were diluted appropriately with RIPA buffer to normalize protein concentrations for all samples per experiment. SDS-PAGE sample buffer and reducing agent (NuPAGE, Life Technologies) were added to samples, boiled and centrifuged at max speed for 30 seconds. Samples were resolved by SDS-PAGE on 4-12% Bis-Tris NuPAGE gels (Invitrogen). Gels were transferred to nitrocellulose membranes with an iBlot (Invitrogen) and blocked for 45 minutes at room temperature with StartBlock (Pierce). Membranes were probed overnight at 4°C with primary antibodies, washed, and probed with fluorescent- or HRP-conjugated secondary antibodies for 45 minutes. The blots were processed and images acquired on a Fluorchem M Imager (Protein Simple). Images were analyzed by band densitometry (Alpha View SA).

**Antibodies**

All antibodies used for Western blotting were purchased from Cell Signaling; ERK 1/2: mouse L34F12, Phospho-ERK: rabbit Y204, AKT: mouse 4074, Phospho-AKt: rabbit S473. Secondary antibodies were purchased from Invitrogen: goat anti-mouse alexa fluor 546, goat anti-rabbit alexa fluor 430, anti-mouse HRP conjugate, anti-rabbit HRP conjugate.

**Electrochemiluminescence (ECL) /MSD (Meso Scale Discovery) detection**

Differentiated C2C12 myotubes were HRG-treated or vehicle-treated, washed with ice-cold PBS, and lysed and normalized as described above. Cell supernatants were

assayed using a Meso Scale Discovery electrochemiluminescence (ECL) assay as per the manufacturer's instructions for AKT, ERK1/2, GSK3-β, JNK, p-38, and mTOR1/2.

**Histology and cell staining**

C2C12 cell culture followed the same protocol as mentioned previously with the following exception, cells were either plated into fibronectin coated (25μg/mL, Invitrogen) 4-well chamber slides (glass or plastic) or 96-well UV-transmissible plates (Greiner, cell culture treated). 20, 40, or 60μM Laminin-111 (laminin) (Sigma) was added on day 3 of differentiation, at the same time 8ng/mL or 80ng/mL HRG was administered for 48-72 hours. Once the HRG-treatment time course was finished, cells were incubated with alpha-bungarotoxin (α-btx) conjugated to alexa fluor 555, (5μg/mL, Invitrogen) for 1 hour at 37°C, washed with PBS and fixed with 4% paraformaldeyde for 30 minutes at room temperature or cold methanol for 10 minutes on ice. The cells were then washed with PBS and permeabilized with 0.02% Triton X-100 (Sigma) with Hoechst to visualize nuclei (Life Technologies). Chamberslides were washed, dried overnight, and mounted with Prolong Gold Antifade with DAPI and 96-well plates were washed, incubated with Hoechst and left in 150μL of PBS at 4°C until imaged.

**Fluorescent microscopy**

Chamberslides were imaged on a Leica DM4000b fluorescent microscope fitted with a DFC 550 CCD camera with 20x and 40x objectives and analyzed with LAS AF software. Whole chamberslide images were acquired and stitched together using an Image Express and MetaMorph Software (Molecular Devices). 96-well plates were

imaged on an Image Express and processed using Columbus Software (Perkin Elmer) by batch analysis of 16 fields per well n≥3 wells per condition. AChR cluster count, cluster area determination and intensity were calculated by determining a minimum threshold of 70% and identifying clusters through spot detection with area >300nm² and <6000nm² and corrected spot intensity >450 and contrast >0.3 similar to Ball, et al. (Matthew K. Ball, 2013). Statistical analysis of variance was performed using the Students T-test (one-tailed, two sample of unequal variance).

**In-vivo HRG efficacy study**

Three week old *mdx* and WT 10snJ mice were treated three times a week with vehicle (PBS) or 200μg/kg of HRG via intraperitoneal injection: 10 WT + vehicle, 12 *mdx* + vehicle, and 13 *mdx* + 200ug/kg HRG. An effort to exacerbate the mild *mdx* pathology was attempted by submitting the mice to 30 minute treadmill exercise twice a week. The study continued for 3 months and mice were sacrificed and tissues harvested for functional or histological analysis. A time course of HRG-treatments during the animal study is shown in Figure 8.
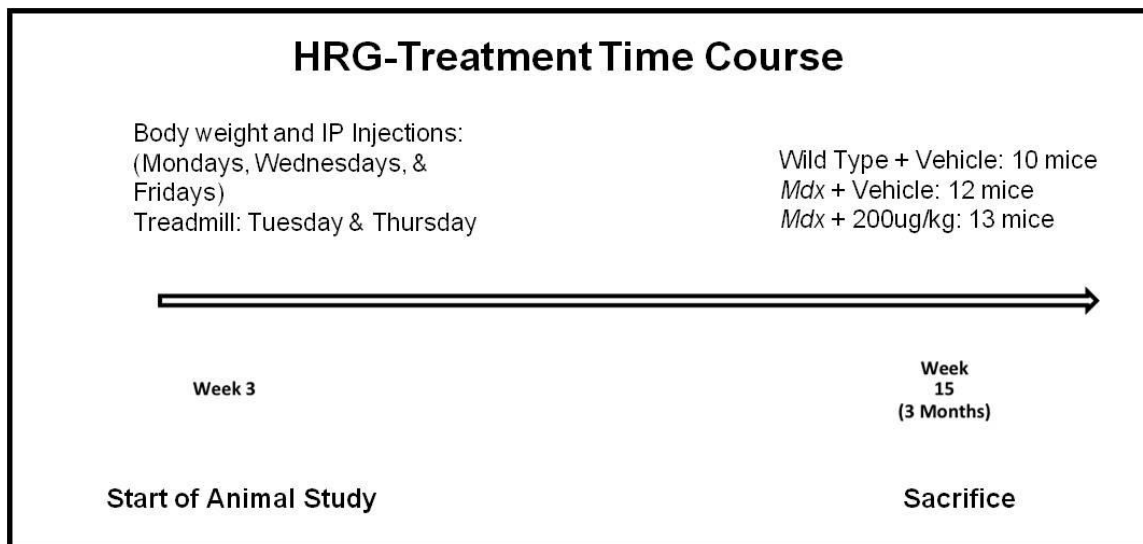
**Figure 8: Time course of HRG-treatment in mice**

**tissue sectioning and immunohistochemistry**

Fresh frozen tibialis anterior muscles (TA) from the HRG efficacy study were warmed to -20°C overnight. Tissues were placed in a cryostat (LEICA CM 1950) for 20 minutes to equilibrate temperature. Several 35µm thick longitudinal sections were transferred onto positively charged slides per condition. Tissues were fixed in 4% paraformaldehyde for 30 minutes followed by three washes with PBS for 5 minutes each. Tissues were subjected to 0.3M glycine to reduce autofluoresence, blocked and permeabilized for 45 minutes with 0.02% Triton X-100 and 0.5% BSA (Sigma), and followed by a series of washes with PBS (Life Technologies). Tissues were stained overnight with primary anti-neurofilament (NF) antibody (Developmental Studies Hybridoma Bank – University of Iowa) at 4°C. Slides were washed and then incubated with alexa fluor 488-conjugated secondary antibody (Life Techniologies) and alexa fluor 555-conjugated α-btx (5µg/mL, Invitrogen) for 45 minutes at room temperature in

blocking buffer. The samples were dried overnight and mounted with Prolong Gold Antifade with DAPI (Invitrogen).

**Epi-fluorescence and confocal microscopy of tissue sections**

Sections were initially imaged & analyzed with a Nikon E800 Upright Epi-fluorescent microscope. Around 48 NMJs were imaged per mouse (n=7) for each condition through fluorescent microscopy. Confocal images were captured with a 40x oil objective and 20-24 Z-stacks, each stack ~1-1.7μm on a Carl Zeiss LSM780 confocal microscope. Around 6 NMJs per mouse (n=4) for each condition were imaged and analyzed by confocal microscopy. Confocal raw data images were extracted with Imaris software and processed using Image J software.

**Results:**

**HRG signaling in myoblasts and myotubes**

The effect of HRG to ameliorate the dystrophic phenotype in *mdx* mice through the up-regulation of utrophin has not been consistently shown as an HRG mechanism of action (Krag et al. 2004 & S. Bell, personal communication). To help identify the mechanism of action by which HRG preserves muscle function, HRG signaling was investigated. It had previously been shown that HRG activates ERK in skeletal muscle and induces gene expression of NMJ proteins (Altiok, Altiok, & Changeux, 1997; Fromm & Burden, 2001; Handschin et al., 2007; Tansey et al., 1996). To confirm previous findings and to establish experimental protocols, ERK activation by HRG was examined.

Mouse C2C12 myoblasts and differentiated myotubes were serum-starved and then treated with varying concentrations of HRG for various times. Activated signaling proteins were analyzed by Western blot with phospho-specific antibodies. Activation was normalized by the ratio of phosphorylated to non-phosphorylated protein signal. HRG activation of ERK in undifferentiated myoblasts is shown in Figure 9. HRG activation of ERK in differentiated myotubes showed a dose dependent response (Figure 10 & 11).
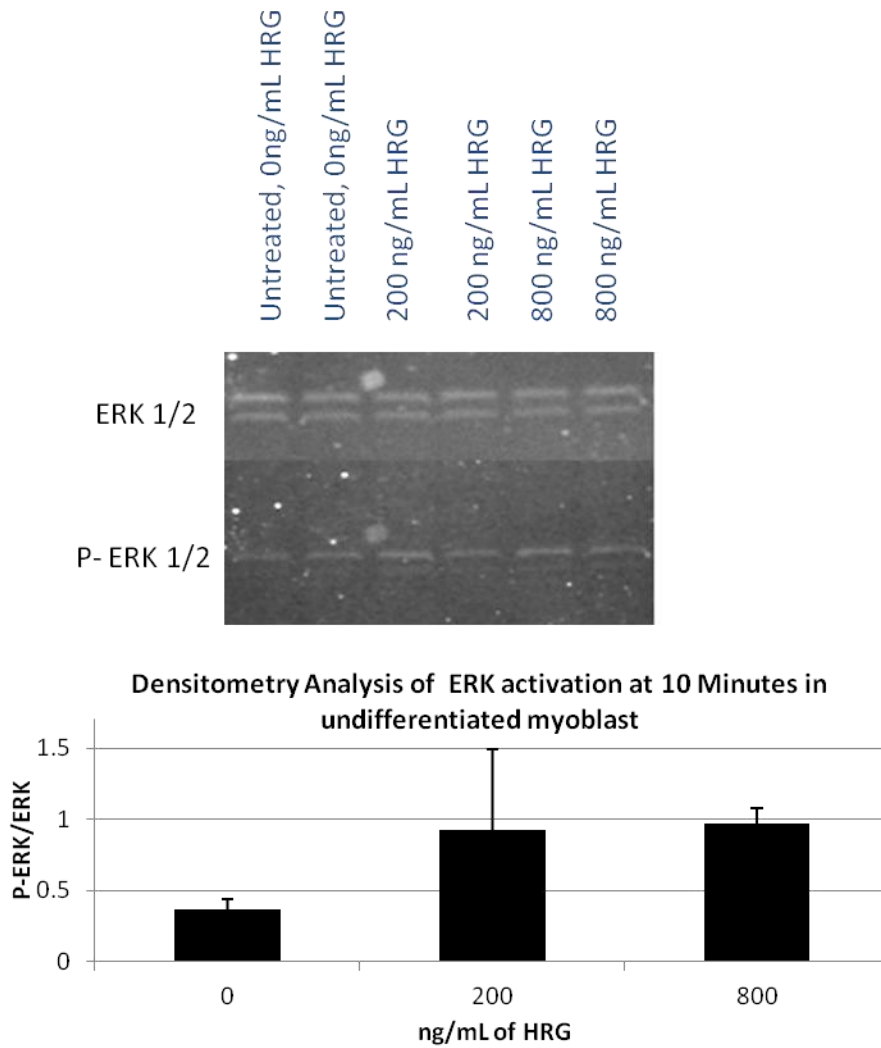
**Figure 9: Activation of ERK in undifferentiated myoblasts**
Western blot and densitometry analysis at 10 minutes showing ERK activation with 200 and 800ng/mL HRG in undifferentiated myoblasts. Each condition was performed in duplicate. These data are representative of 3 experiments.
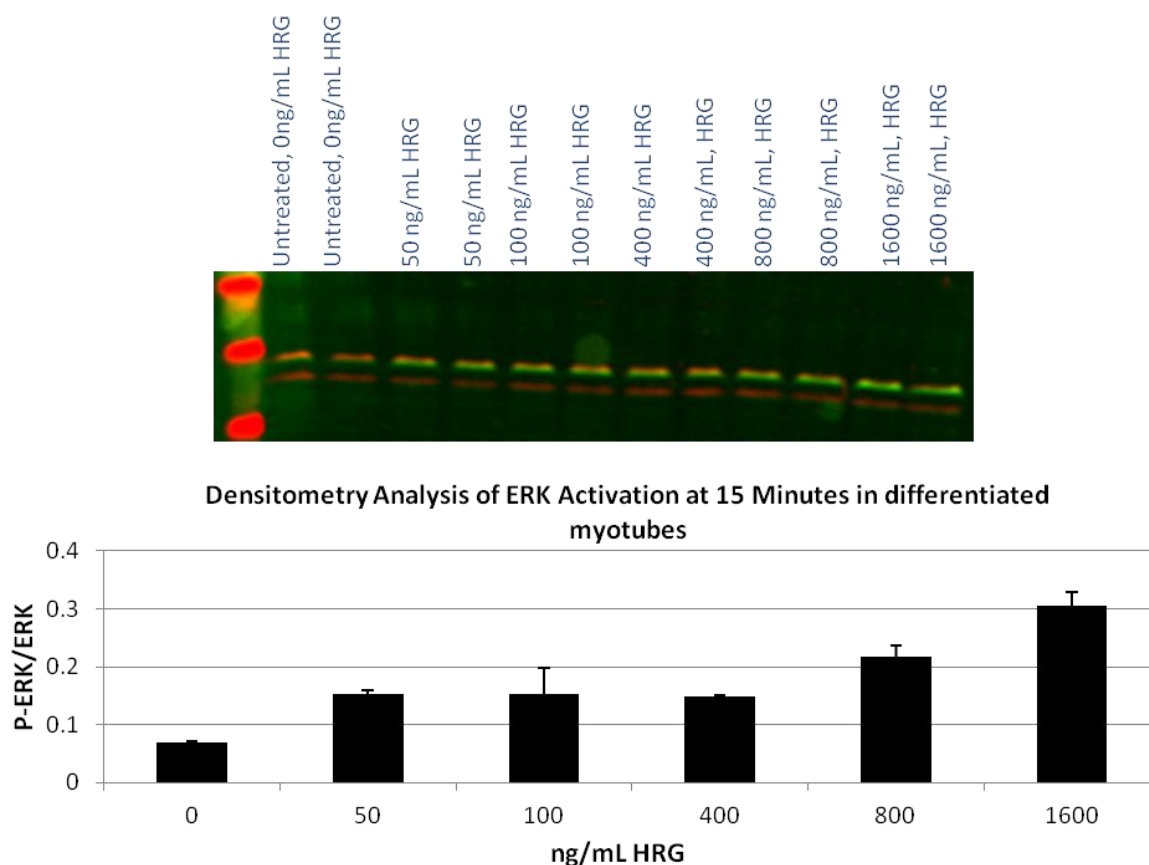
**Figure 10: HRG activation of ERK in differentiated myotubes**
Differentiated myotubes were treated with 0, 50, 100, 400, 800 & 1600ng/mL HRG for 15 minutes. Lysates were analyzed by Western blot and densitometry analysis. Each condition was performed in duplicate. These data are representative of 3 experiments.

The HRG-mediated activation of ERK confirmed previous findings of ERK activation in C2C12 cells. Since ERK activation occurred in undifferentiated myoblasts and differentiated myotubes, a direct effect, specific to differentiated muscle myotubes, could not be linked to ERK activation following HRG treatment. Other MAP Kinase pathways, JNK (c-Jun N-terminal kinase) and p38 were examined. JNK and p38 are crucial for cell survival and regulate cell proliferation (Bernet et al., 2014; Sakamoto & Goodyear, 2002). In order to simplify the MAP Kinase pathway analysis into a single

experiment, ERK, JNK and p38 protein and their phospho-protein isoforms were assayed

in a single ECLA experiment (n=2 biological replicates per experiment, n=6 experimental

replicates). The results confirmed a HRG dose dependent activation of ERK, peaking at

10 minutes (Figure 11), but revealed no activation of JNK (Figure 12) or p38 (Figure 13)

in differentiated C2C12 myotubes..
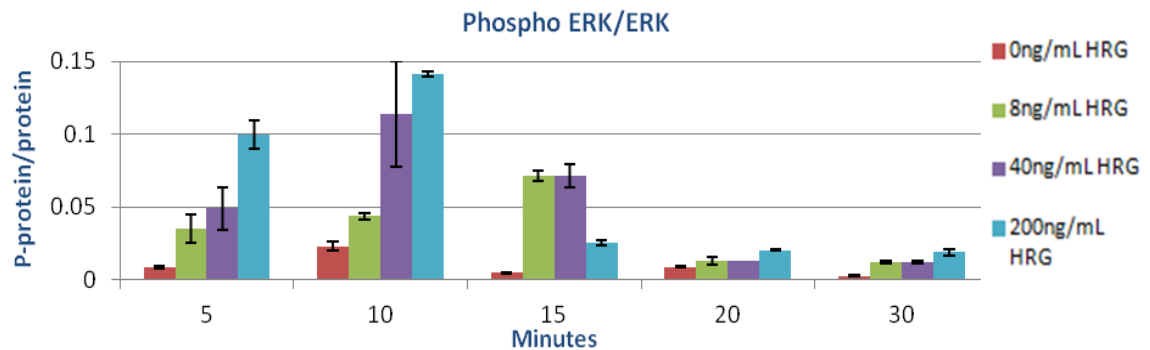


**Figure 11: HRG dose dependent ERK activation**
ECLA showing that HRG activation of ERK peaks by 10 minutes at 40 and 200ng/mL HRG.
Data are the average of duplicates and representative of 6 independent experiments.



**Figure 12: HRG does not activate JNK**
ECLA showing that HRG does not appear to activate JNK between 5 and 30 minutes at 8,
40, or 200ng/mL HRG. Data are the average of duplicates and representative of 6

independent experiments.



**Figure 13: HRG does not activate p38**
ECLA showing that HRG does not appear to activate p38 between 5 and 30 minutes at 8, 40, or 200ng/mL HRG. Data are the average of duplicates and representative of 6 independent experiments.

AKT has been shown to be important in muscle, and HRG activation of AKT has previously been demonstrated in non-muscle cells *in vitro.* However, it is not clear if HRG activation of AKT in dystrophic muscle would be beneficial. AKT is linked to muscle cell survival, differentiation through the stimulation of growth factors, fiber type switching, and glucose metabolism (Blaauw et al., 2009; Blaauw et al., 2008; Schiaffino & Mammucari, 2011). To test the activation of AKT in muscle-derived cells, C2C12 myoblasts and myotubes were treated with HRG as in the MAP kinase experiments above. Dose-dependent activation of AKT was detected following HRG-treatment. However, unlike ERK, AKT was only activated in differentiated myotubes (Figure 15) and not myoblasts (Figure 14). This myotube specific effect could mean that downstream events from AKT activation might contribute to the prevention of muscle dystrophy (Bodine et al., 2001).
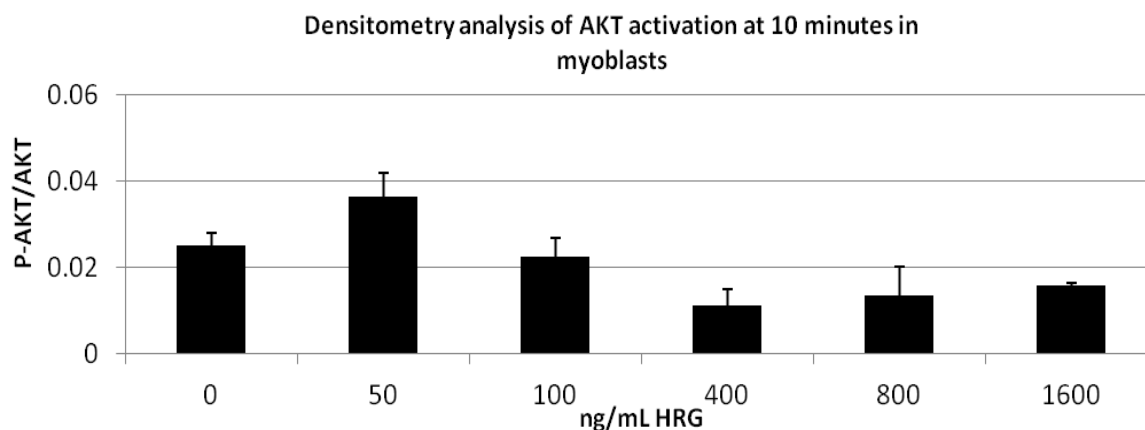
**Figure 14: Activation of AKT in undifferentiated C2C12 myoblasts**
Myoblasts were treated with 0, 50, 100, 400, 800 & 1600ng/mL HRG for 10 minutes. Lysates were analyzed by Western blot and densitometry analysis. Each condition was performed in duplicate. These data are representative of 3 experiments.
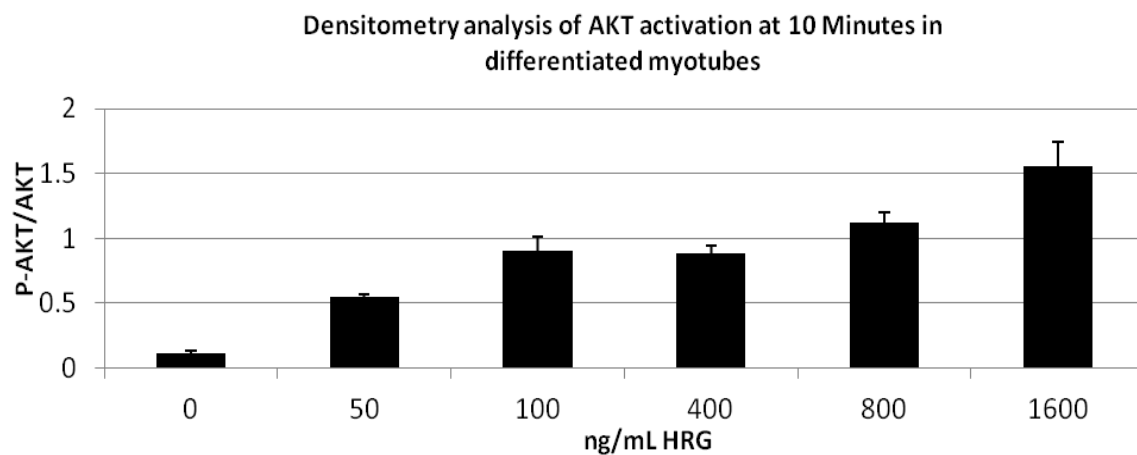


**Figure 15: Activation of AKT in differentiated C2C12 myotubes**
Differentiated myotubes were treated with 0, 50, 100, 400, 800 & 1600ng/mL HRG for 10 minutes. Lysates were analyzed by Western blot and densitometry analysis. Each condition was performed in duplicate. These data are representative of 3 experiments.

As AKT activation was differentially activated in C2C12 myotubes, downstream signaling might be important for potential AKT-mediated benefits. Downstream pathways of AKT were investigated to explore HRG signaling. GSK-3β, a substrate of AKT, was investigated because of its involvement in cell fate, development, and glycogen synthesis (Wojtaszewski, Nielsen, Kiens, & Richter, 2001). It was previously shown that the activation of p70s6k from AKT was linked to the alleviation of muscular dystrophy by promoting muscle cell survival (Boppart, Burkin, & Kaufman, 2011). In order to simplify analysis of downstream AKT signaling, AKT, GSK-3β and p70s6K protein and phospho-protein isoforms were assayed in a single ECLA experiment (n=2 biological replicates per experiment, n=6 experimental replicates). While these experiments confirmed activation of AKT between 5 and 30 minutes (Figure 16), it was observed that HRG did not activate either GSK-3β (Figure 17) or p70s6K (Figure 18) up to 90 minutes following HRG treatment (data not shown). Although the GSK-3β data at 5 and 10 minutes suggested there might have been activation, in six additional experiments, this observation was never repeated.
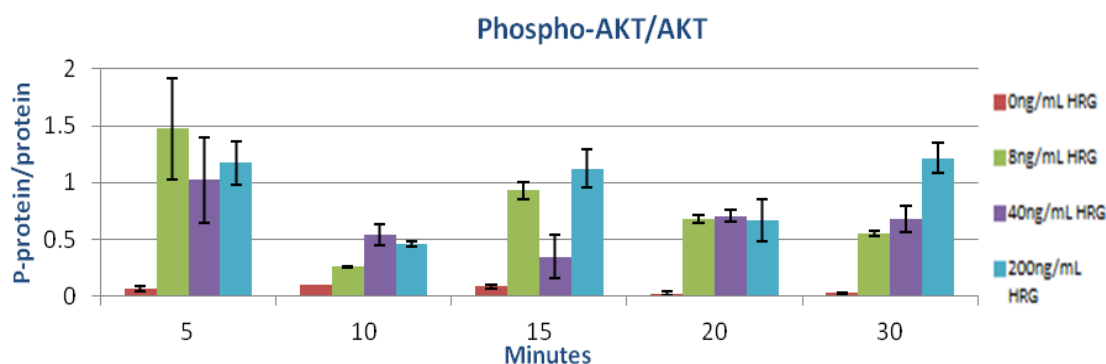


**Figure 16: HRG dose activation of AKT in C2C12 myotubes**
ECLA showing that HRG activation of AKT peaks by 5 minutes at 8, 40, and 200ng/mL

HRG, but remains active for at least 30 minutes. Data are the average of duplicates and representative of 6 independent experiments.
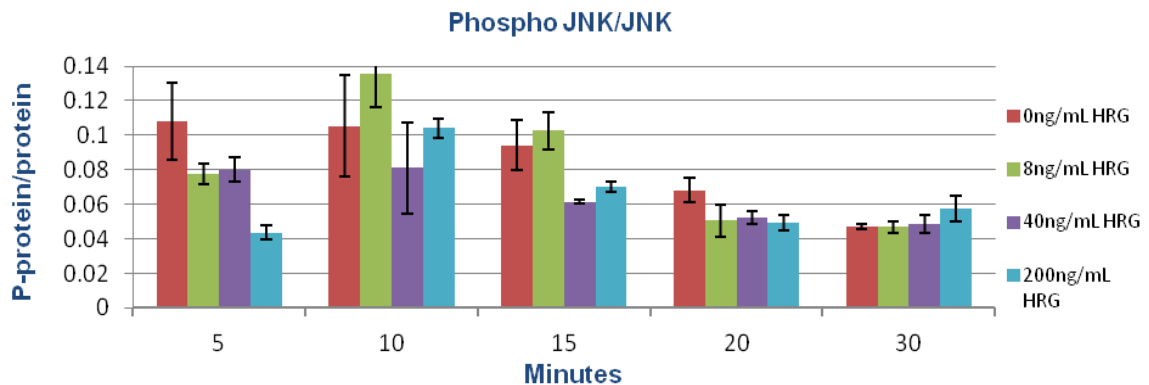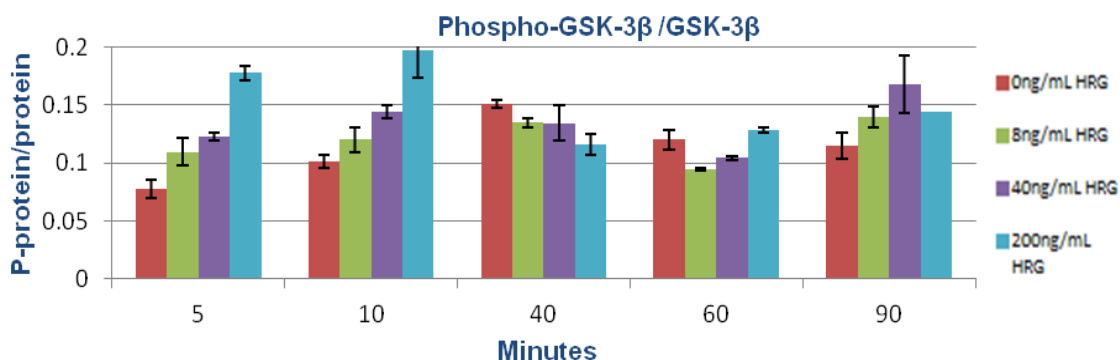


**Figure 17: HRG does not activate GSK-3β**
ECLA showing that HRG does not appear to activate GSK-3β between 5 and 90 minutes at 8, 40, or 200ng/mL HRG. Data are the average of duplicates and representative of 6 independent experiments.
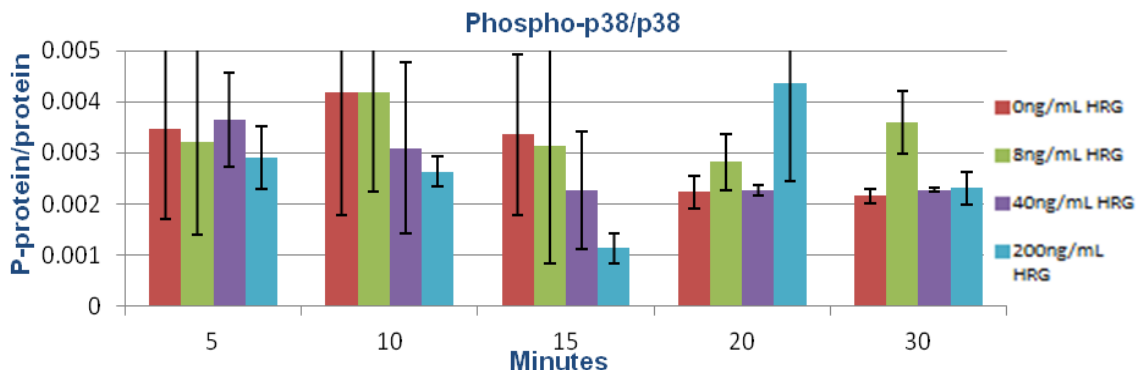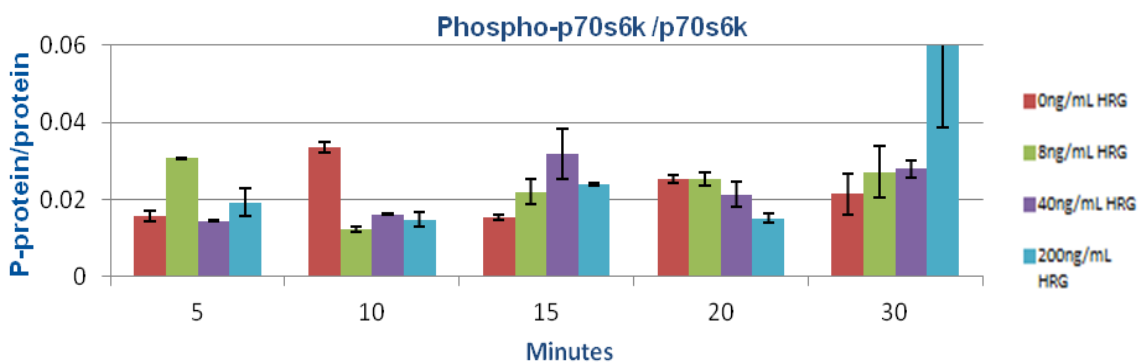


**Figure 18: HRG does not activate p-70s6k**
ECLA showing that HRG does not appear to activate p70s6k between 5 and 30 minutes at 8, 40, or 200ng/mL HRG. Data are the average of duplicates and representative of 6 independent experiments.

mTOR, another protein downstream of AKT and linked to the prevention of muscle atrophy and mitochondrial health, was investigated (Bodine et al., 2001). mTOR showed no activation following HRG treatments up to 90 minutes in an ECLA (Figure 19), which was confirmed by Western blot analysis (data not shown). The results were

unexpected as mTOR is responsible for cell survival and is a common target of AKT signaling (Bodine et al., 2001). It is important to keep in mind that the signaling experiments were performed in C2C12 myotubes *in vitro,* not muscle tissue *in vivo.* The C2C12 myotubes may be an incomplete model for signaling in muscle.
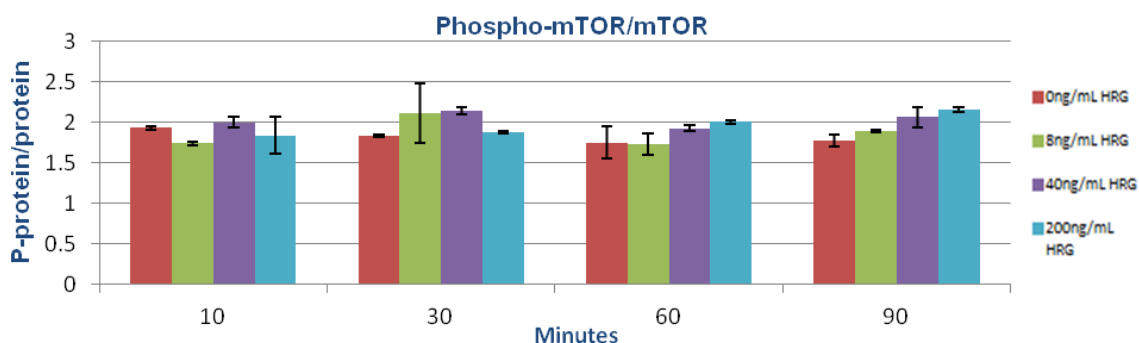


**Figure 19: HRG does not activate mTOR**
ECLA showing that HRG does not appear to activate mTOR between 10 and 90 minutes at 8, 40, or 200ng/mL HRG. Data are the average of duplicates and representative of 6 independent experiments.

**HRG effects on AChR clusters in C2C12 myotubes**

The activation of ERK by HRG has been shown to induce the expression of several NMJ proteins including AChR (Handschin et al., 2007). It has also been shown that laminin induces AChR clustering in differentiated C2C12 myotubes, and dystrophin-deficiency contributes to the loss of AChR cluster organization (Personius & Sawyer, 2005; Sugiyama, Glass, Yancopoulos, & Hall, 1997). The effects of HRG signaling on laminin-induced AChR clustering and morphology in differentiated C2C12 myotubes were examined by histological analysis. AChR clustering occurred spontaneously in differentiated myotubes (Figure 20A). The addition of laminin induced or accelerated AChR clustering in C2C12 cells plated on fibronectin-coated slides (Figure 20B), while

HRG-treatment reduced AChR clustering (Figure 20C). C2C12 myotubes, which were treated with HRG and laminin at the same time, appeared to show an effect on the spatial organization of AChR clusters. It was observed that HRG appeared to influence the location of laminin-induced AChR clusters with some clusters having a central localization (Figure 20D) compared to only being on an edge, whether a cell-cell or cell-matrix interaction (Figure 20B). This phenomenon indicated HRG-treated Laminin induced AChR clusters might be more matrix-cell independent. In HRG-treated myotubes, the α-btx stain appeared dimmer in laminin-induced clusters (Figure 20D) while having a brighter and more diffuse membrane staining in the absence of laminin (Figure 20C), suggesting a greater dispersal of AChRs. These results are similar to observations in the scientific literature (Trinidad & Cohen, 2004).
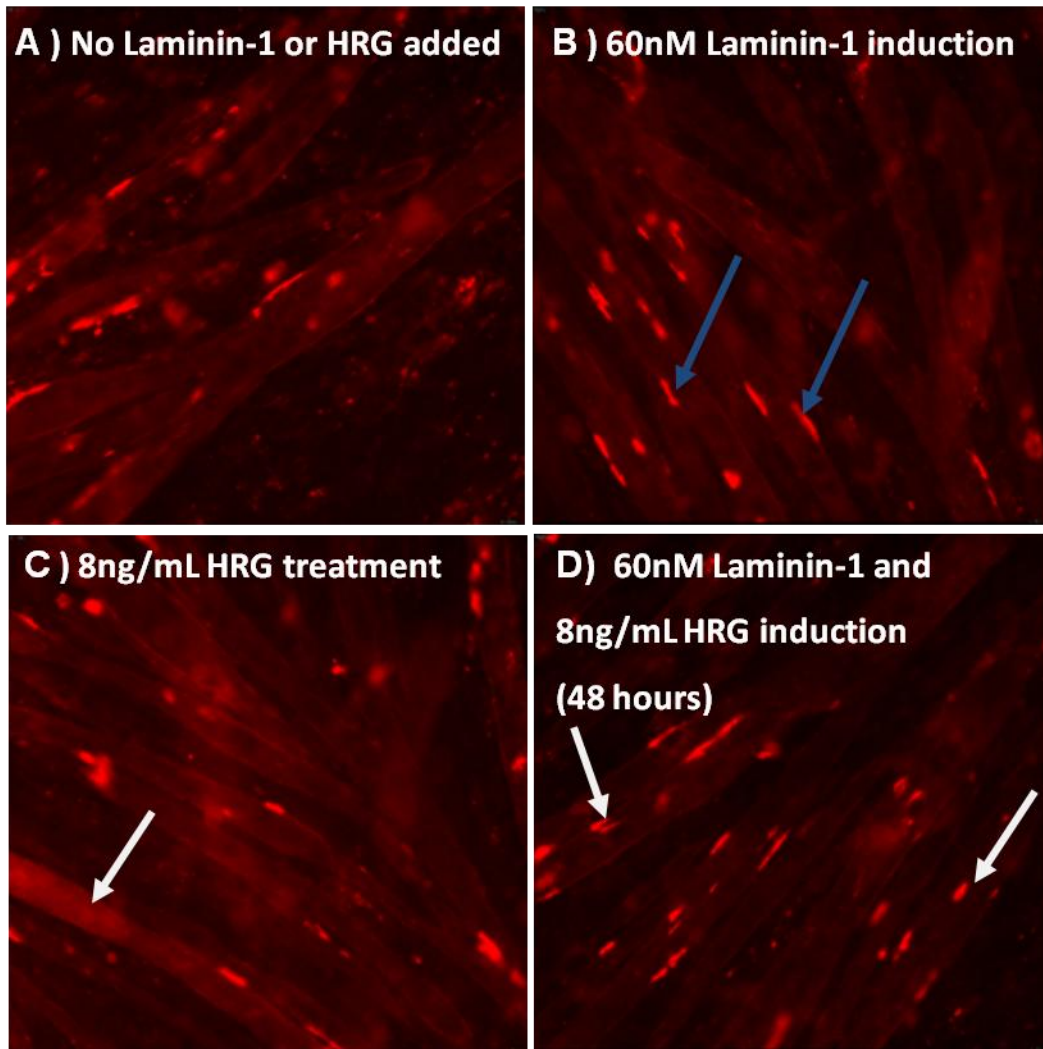
**Figure 20: HRG modulated AChR clustering in differentiated C2C12 myotubes**
Epi-fluorescence microscopy of a-btx stained C2C12 differentiated myotubes on fibronectin-coated slides.  No Laminin-1 or HRG added (A), 60nM Laminin-1 (B), 8ng/mL HRG induction (C) (D) 60nM Laminin-1 and 8ng/mL HRG induction (D). Note: Blue arrows represent AChR clustering, white arrors shows AChRs dispersed throughout myotubes or centralized cluster.

To quantitate the observations made subjectively on AChR clustering in C2C12 myotubes plated on fibronectin-coated slides, C2C12 cells were plated onto 96 well UV-transmissable plates for high content analysis.  The following conditions were tested at

24, 48, 72 and 96 hours with the number of wells indicated (n): No laminin+no HRG (n=12); no laminin+8ng/mL HRG (n=6); no laminin+80ng/mL HRG (n=6); 20nM laminin+no HRG (n=6); 40nM laminin+no HRG (n=6); 60nM laminin+no HRG (n=6); 20nM laminin+8ng/mL HRG (n=3); 40nM laminin+8ng/mL HRG (n=3); 60nM laminin+8ng/mL HRG (n=3); 20nM laminin+80ng/mL HRG (n=3); 40nM laminin+80ng/mL HRG (n=3); 60nM laminin+80ng/mL HRG (n=3). Sixteen fields from each well were imaged by an Image Express (Molecular Devices) for a minimum of 48 images per condition. Each field contained 2-12 myotubes or fractions of myotubes. The images were analyzed in batch using Columbus software (Perkin Elmer) to identify clusters as detailed in Materials and Methods. AChR clusters were identified, counted, and the cluster area and intensity determined. The intensity value is relative to the concentration of AChRs found in clusters while the area is indicative of cluster size. At 24 hours following HRG-treatments, there was no significant difference in the trending of AChR clustering (data not shown). However, HRG had a dose-dependent effect on the laminin-induced AChR clusters on cluster number, total cluster intensity (Figure 21A) and mean cluster area (Figure 21B) at 48 hours. The addition of 80ng/mL HRG reduced the total number of 20nM and 60nM laminin-induced clusters/well by 34% ($p < 0.02$) and 23% ($p = 0.05$), respectively. While HRG treatment reduced the total cluster intensity of laminin-induced clusters, only at 80ng/mL HRG and 60nM laminin-1 was the effect statistically significant ($p < 0.01$). Similarly, HRG significantly reduced the mean cluster size (area) at 80ng/mL for the 60nM laminin-induced clusters ($p < 0.01$). AChR clustering was also examined at 72 hours (Figure 22) and, similar to the observations made at 24 hours, no trend was

observed. The dose-dependent HRG-effects appeared to diminish by 72 hours. No

attempt was made to determine localization of AChR clusters as that appeared to be

beyond the capacity of the algorithm for the staining protocol that was performed.
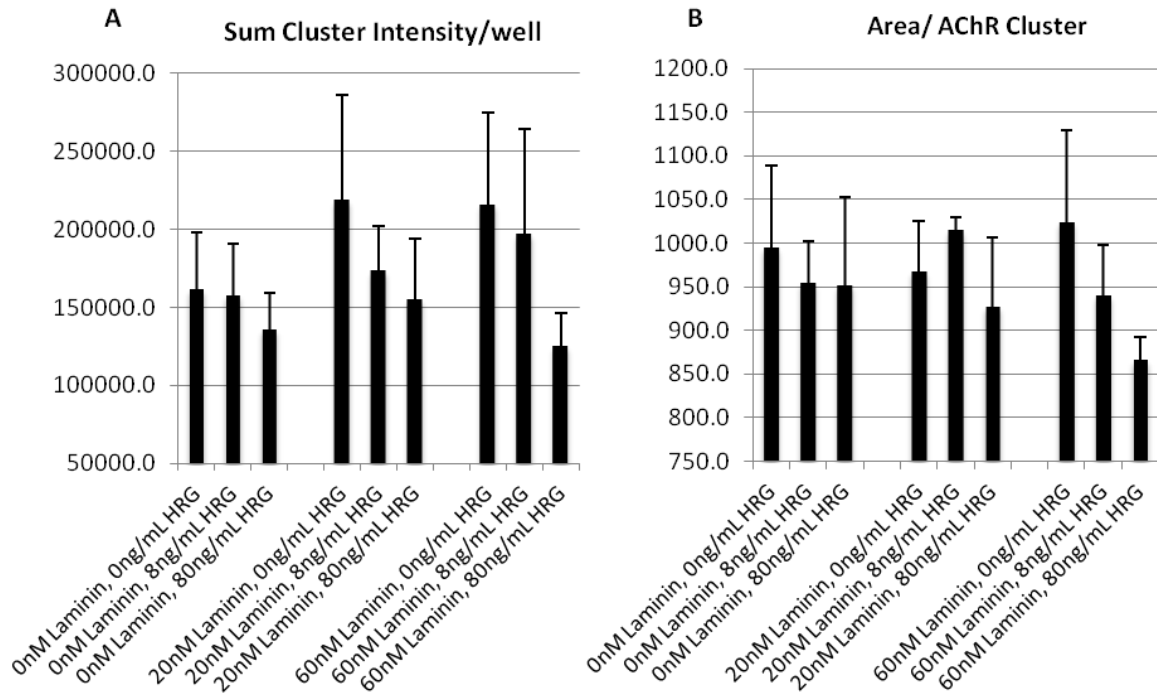


**Figure 21: AChR clustering after a 48 hour HRG treatment**
AChR clustering count in differentiated C2C12 myotubes on the fifth day of
differentiation with a 48 hour HRG treatment of 8 and 80ng/mL HRG on spontaneous
and laminin-induced AChR cluster formation showing (A) sum cluster intensity/well and
(B) area/AChR cluster. Error bars depict standard deviation of well averages.
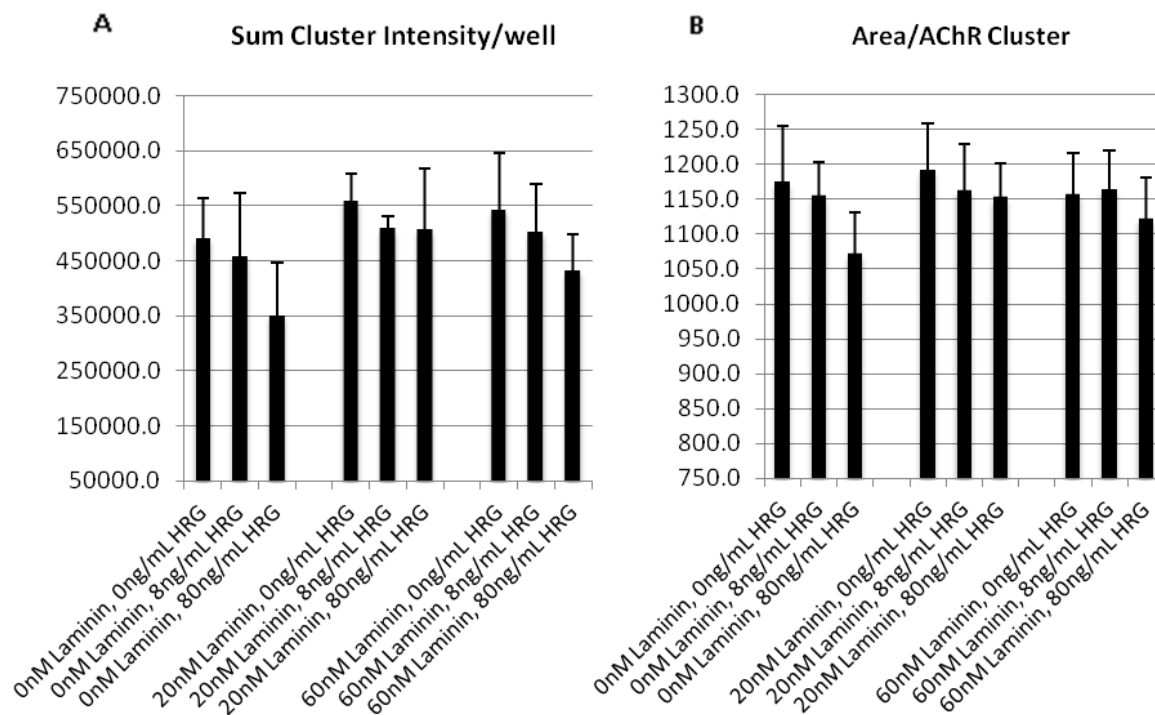
**Figure 22: AChR clustering after a 72 hour HRG treatment**
AChR clustering count in differentiated C2C12 myotubes on the sixth day of differentiation with a 72 hour HRG treatment of 8 and 80ng/mL HRG showing (A) sum cluster intensity/well and (B) area/AChr cluster. Error bars depict standard deviation of well averages.

**Effects of HRG on NMJ formation *in vivo***

Our observation of HRG activation of ERK, its documented downstream effects on NMJ gene transcription, and our observation of AChR cluster reorganization led us to examine whether HRG might affect NMJ morphology in the *mdx* mouse. NMJs, which are shown to be defective in *mdx* mice (Figure 6), might benefit from ERK and/or AKT signaling. In order to understand the effect HRG has on NMJ formation, the TA muscles from vehicle and HRG-treated *mdx* mice and vehicle-treated wild type (WT) mice were examined by staining with alexa fluor 555-conjugated α-btx, which stains the AChR on the muscle side of the NMJ. Figure 23 shows WT, *mdx* and HRG-treated *mdx* NMJs. The

vast majority of the WT NMJs examined in this study were comparable to those found in

the scientific literature showing a continuous pretzel-like NMJ (Figure 22A and 23A)

(Arnold et al., 2014; Bolliger et al., 2010). The *mdx* mouse had discontinuous NMJ

formation, which is commonly referred to in the literature as Island-like or bouton

formation. The NMJ islands in HRG-treated *mdx* tissue appear to be more conjoined

(Figure 23C and 24) when compared to the random, bouton *mdx* NMJs (Figure 23B and

24). HRG treatment did not completely restore the *mdx* NMJ phenotype to WT, but HRG

treatment did show a partial restoration of NMJ morphology.
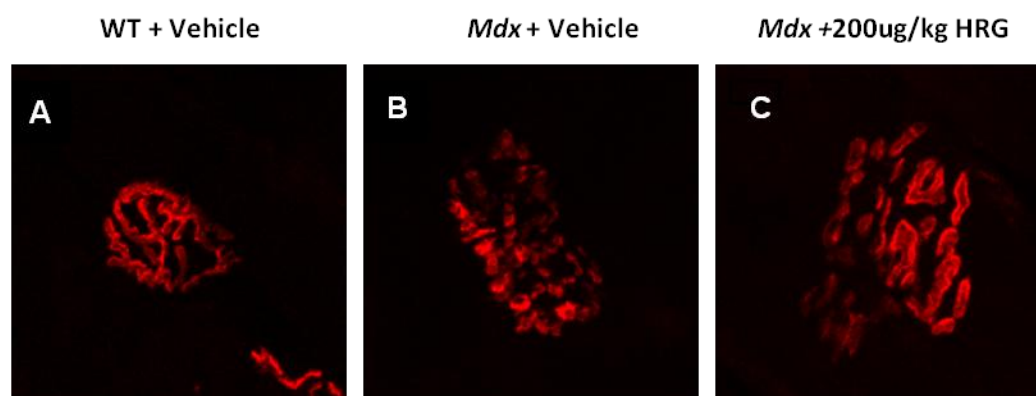


**Figure 23: General NMJ morphology**
WT 10snJ mice show healthy pretzel-like NMJs (A) while mdx mice show a
discontinuous,  island-like NMJs (B), and 200ug/kg HRG-treated mdx mice show a
partially restored morphology (C).

To further understand any effects HRG might have beyond changes in overall

NMJ morphology, the interaction between the nerve terminal and muscle were

analyzed by co-staining with an antibody to neurofilament (NF) protein found in the

axon termini and alexa fluor 555-conjugated α-btx to label AChRs on the muscle fiber.

Through Epi-fluorescence microscopy, it was observed that in some NMJs the axons of nerve terminals had higher integration throughout the NMJ when *mdx* mice were treated with HRG than compared to the vehicle-treated *mdx* mice (data not shown) and was confirmed through confocal microscopy (Figure 24A). Confocal microscopy was used to determine a more precise location of axonal and AChR interactions. HRG-treated tissues showed a higher nerve terminal integration with AChR throughout the NMJ, as though the nerve was trying to compensate for the NMJ malformation by reaching out to each island when compared to the vehicle-treated *mdx* mouse muscle, where nerve terminal integration appeared very inconsistent.
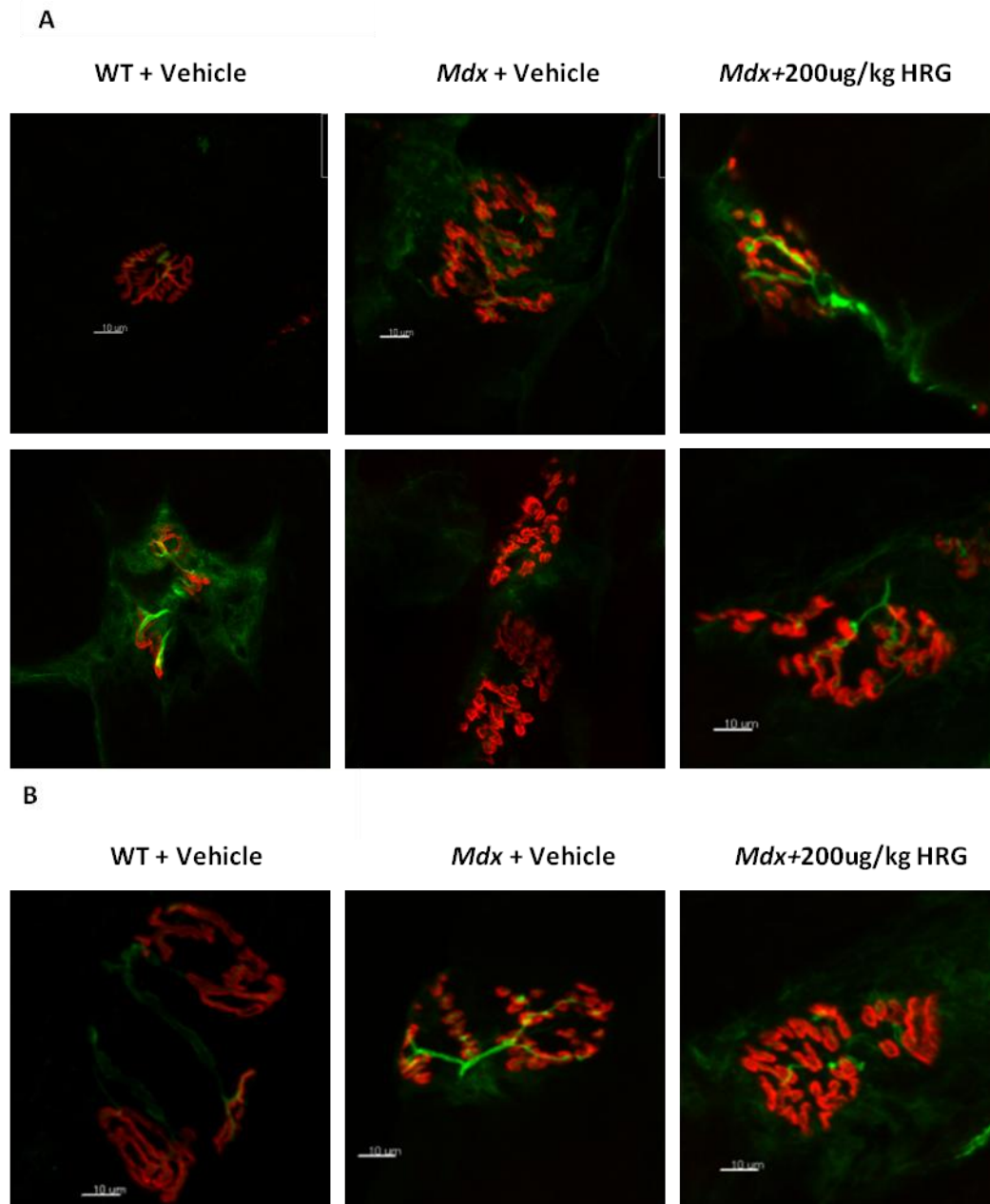
**Figure 24: HRG effects on AChR and axonal interactions**
NMJs are shown in red and the axon (nerve terminal) is shown in green. Confocal microscopy showing location of axonal and NMJ interaction in WT (Left), *mdx* + vehicle (middle), and 200µg/kg HRG-treated (Right) NMJs. HRG effects on AChR and axonal interactions showing increased integration (A), however, HRG effects on NMJ and axonal interactions are not consistent (B). Data are representative of 6 NMJs analyzed per mouse, 4 mice per condition.

It appeared that HRG-treated mice showed a higher integration of nerve terminals throughout the NMJ compared to the vehicle. Yet, the effect seen from HRG-treatments was not consistent among all NMJs (24B), possibly due to incomplete biodistribution of HRG. This data led us to the possible conclusion that HRG might modify NMJ formation and possibly influence nerve terminal migration to better adapt to signaling in *mdx* NMJs and improve muscle function through increased excitation contraction coupling.

**Results summary**

In summary, through *in vitro* and *in vivo* experiments, mechanisms of action for HRG-mediated effects on muscle were examined. HRG signaling *in vitro* provided confirmation of ERK activation in undifferentiated myoblasts and differentiated myotubes, whereas AKT activation was observed only in differentiated myotubes. There was no clear evidence of JNK, p38, GSK-3β, p70s6K or mTOR activation. Due to HRG activation of ERK and NMJ gene up-regulation as a result of ERK signaling, AChR clustering in differentiated C2C12 myotubes was investigated and found to have a dose-dependent decrease in AChR cluster area and intensity. NMJ morphology was examined *in vivo* following the administration of HRG to *mdx* mice. NMJs in *mdx* mice treated with HRG showed a partial restoration in NMJ morphology. Co-staining AChRs of HRG-treated and non-treated *mdx* mice with a NF antibody provided evidence that HRG increased NMJ integration between the nerve terminal and AChRs, which could lead to improved excitation contraction coupling resulting in improved muscle function.

**Discussion:**

**A downstream signaling mechanism has not yet been determined**

The HRG signaling pathway in muscle has not been completely elucidated. In differentiated C2C12 myotubes, HRG activates AKT and ERK, but surprisingly does not activate mTOR, JNK, p-38, p70s6k, or GSK-3β, which are downstream of AKT and ERK or represent parallel pathways. Downstream signaling of ERK in C2C12 myoblasts and myotubes have been thoroughly studied and, for the most part, point to the induction of AChR, utrophin and many other NMJ-associated genes. The results presented here indicate that the ERK activation observed in C2C12 cells may translate to the reorganization of laminin-induced AChR clusters *in vitro* and the improvement of NMJ formation *in vivo*. Although the result could be predicted based on literature, this study is the first to make the direct observation of HRG affecting the NMJ of *mdx* mice *in vivo*. Although AKT is activated *in vitro* in C2C12 myotubes, the effects of this activation were not determined in this study.

HRG activation of AKT did not lead to the activation of GSK-3β, mTOR, or p70s6k, downstream mediators of AKT signaling. This result was surprising and indicates that there may be a separate pathway activated by HRG through AKT. More likely, it could mean that C2C12 cells are not a surrogate for muscle when examining AKT signaling. AKT signaling is responsible for fiber-type switching, muscle fiber hypertrophy and decreased muscle apoptosis. However, it was not possible to examine these effects *in vitro.* These responses to AKT activation could be mediated by mTOR, which is responsible for cell survival and has been shown to prevent muscle atrophy *in vivo,* so it

was surprising to find HRG did not activate mTOR (Bodine et al., 2001). HRG activation of AKT was specific to myotubes and might point to a different outcome for more mature muscle upon the administration of HRG. Due to the limitations in the C2C12 cell culture model, investigation of AKT and mTOR signaling *in vivo* may yield different results.

**HRG decreases AChR clustering in C2C12 differentiated myotubes**

ERK activation has been associated with NMJ-associated gene expression. As HRG activated ERK, it might be expected that an effect on AChR clusters would be observed. What was surprising was the nature of the HRG effects. One would expect that HRG-treatments might increase AChR clusters as HRG treatment has been shown to increase total AChR protein. What was observed in this study, however, was not an increase in AChR clusters, but a decrease in number, area, and intensity of the Laminin-induced AChR clusters at 48 hours. There was an increase in overall clusters in the 72 hour time point compared to the 48 hour time point. However, the HRG effects seemed to diminish by 72 hours. Interestingly, there did not seem to be a trend in AChR clusters treated with only laminin.

When myotubes were not subjected to HRG or laminin treatments, AChR clustering is spontaneous as shown in Figure 20A. AChRs in myotubes treated with HRG (Figure 20C) appeared to be more dispersed throughout the membrane when compared to treatment of cells with Laminin-1 (Figure 20B). Further investigation could focus on whether the HRG-treated AChR cluster migration (differences in spatial orientation

throughout the myotubes when compared to just the Laminin-1 treatment) observed in cell culture translates to the partial repair in NMJs as seen *in vivo (*Figure 23 and 24).

**HRG modifies NMJ morphology to improve axonal integration**

It was observed that AChR clusters not only decrease in the presence of HRG, but clusters were not restricted to the edges of myotubes suggesting enhanced remodeling, dispersion, and/or plasticity resulting from HRG signaling; this finding led to the investigation of HRG-effects on NMJ formation. HRG partially repaired NMJ morphology, reducing the bouton formation and increasing contiguous α-btx staining. It is unclear whether this observation is a direct result of ERK activation, but many studies have indicated a role for ERK activation by HRG in the control of NMJ gene regulation and would support an effect mediated through ERK. It would be interesting to evaluate correlations between ERK activation and partial repair of NMJ following HRG-treatments. Although HRG may appear to modify NMJ formation and increase axonal and NMJ integration, these observations are not consistent between all NMJs or mice. As some mice responded better to HRG treatments (S. Bell, personal communication), this could be due to the variability of the *mdx* model, bioavailability of HRG to all muscle tissue or a combination of both factors. Further analysis by BioMarin of other tissues could help resolve these issues.

**Conclusion:**

It has been observed that HRG can ameliorate the dystrophic phenotype in mdx mice. However, the mechanism of action of HRG had not been identified. In fact the proposed mechanism of utrophin induction was not reproduced by BioMarin researchers. The goal of this thesis was to explore and/or determine alternative mechanisms of action that would explain the benefits of HRG treatment on dystrophic muscle. Although AKT activation in C2C12 cells possibly created more questions than were answered, the reproducible activation of ERK and the body of literature linking ERK to the regulation of NMJ genes supported the examination of HRG effects on AChR clustering and NMJ formation. It had previously been observed that AChR total protein increases upon HRG treatment. However, an increase in AChR clusters was not observed. Just the opposite was observed: fewer clusters, less area per cluster and at a lower intensity indicating fewer AChR/cluster. Another observation was that AChR clusters were not restricted to the edges of tubes, suggesting enhanced remodeling or plasticity was induced by HRG treatment. When NMJs were analyzed in TA muscle from HRG-treated mdx mice, an improvement in NMJ morphology and neurofilament interaction was observed, supporting a potential role of HRG in promoting NMJ plasticity and repair of defective mdx NMJ. This improved NMJ structure may improve excitation contraction coupling to restore muscle function or prevent muscle damage. Although not definitive, this thesis goes a long way towards suggesting a novel mechanism of action for HRG in the amelioration of the dystrophic phenotype associated with dystrophin deficiency through the repair of NMJ and/or restoration of

NMJ function. The evidence reported here supports a role for HRG involvement in NMJ plasticity and repair to improve excitation contraction coupling in *mdx* mice as a possible mechanism of action to preserve muscle function in a DMD animal model.

References:

Altiok, N., Altiok, S., & Changeux, J. P. (1997). Heregulin-stimulated acetylcholine receptor gene expression in muscle: requirement for MAP kinase and evidence for a parallel inhibitory pathway independent of electrical activity. *Embo j, 16*(4), 717-725. doi: 10.1093/emboj/16.4.717

Archer, J. D., Vargas, C. C., & Anderson, J. E. (2006). Persistent and improved functional gain in mdx dystrophic mice after treatment with L-arginine and deflazacort. *Faseb j, 20*(6), 738-740. doi: 10.1096/fj.05-4821fje

Arnold, A. S., Gill, J., Christe, M., Ruiz, R., McGuirk, S., St-Pierre, J., . . . Handschin, C. (2014). Morphological and functional remodelling of the neuromuscular junction by skeletal muscle PGC-1alpha. *Nat Commun, 5*, 3569. doi: 10.1038/ncomms4569

B J Petrof, J. B. S., H H Stedman, A M Kelly, and H L Sweeney. (1993). Dystrophin protects the sarcolemma from stresses developed during muscle contraction. *Proc Natl Acad Sci U S A, 90*(8), 3710-3714.

Barros, C. S., Calabrese, B., Chamero, P., Roberts, A. J., Korzus, E., Lloyd, K., . . . Muller, U. (2009). Impaired maturation of dendritic spines without disorganization of cortical cell layers in mice lacking NRG1/ErbB signaling in the central nervous system. *Proc Natl Acad Sci U S A, 106*(11), 4507-4512. doi: 10.1073/pnas.0900355106

Basu, U., Gyrd-Hansen, M., Baby, S. M., Lozynska, O., Krag, T. O., Jensen, C. J., . . . Khurana, T. S. (2007). Heregulin-induced epigenetic regulation of the utrophin-A promoter. *FEBS Lett, 581*(22), 4153-4158. doi: 10.1016/j.febslet.2007.07.021

Bernet, J. D., Doles, J. D., Hall, J. K., Kelly Tanaka, K., Carter, T. A., & Olwin, B. B. (2014). p38 MAPK signaling underlies a cell-autonomous loss of stem cell self-renewal in skeletal muscle of aged mice. *Nat Med, 20*(3), 265-271. doi: 10.1038/nm.3465

Bezakova, G., & Ruegg, M. A. (2003). New insights into the roles of agrin. *Nat Rev Mol Cell Biol, 4*(4), 295-308. doi: 10.1038/nrm1074

Blaauw, B., Canato, M., Agatea, L., Toniolo, L., Mammucari, C., Masiero, E., . . . Reggiani, C. (2009). Inducible activation of Akt increases skeletal muscle mass and force without satellite cell activation. *Faseb j, 23*(11), 3896-3905. doi: 10.1096/fj.09-131870

Blaauw, B., Mammucari, C., Toniolo, L., Agatea, L., Abraham, R., Sandri, M., . . . Schiaffino, S. (2008). Akt activation prevents the force drop induced by eccentric contractions in dystrophin-deficient skeletal muscle. *Hum Mol Genet, 17*(23), 3686-3696. doi: 10.1093/hmg/ddn264

Bodine, S. C., Stitt, T. N., Gonzalez, M., Kline, W. O., Stover, G. L., Bauerlein, R., . . . Yancopoulos, G. D. (2001). Akt/mTOR pathway is a crucial regulator of skeletal muscle hypertrophy and can prevent muscle atrophy in vivo. *Nat Cell Biol, 3*(11), 1014-1019. doi: 10.1038/ncb1101-1014

Bolliger, M. F., Zurlinden, A., Luscher, D., Butikofer, L., Shakhova, O., Francolini, M., . . . Sonderegger, P. (2010). Specific proteolytic cleavage of agrin regulates maturation of the neuromuscular junction. *J Cell Sci, 123*(Pt 22), 3944-3955. doi: 10.1242/jcs.072090

Boppart, M. D., Burkin, D. J., & Kaufman, S. J. (2011). Activation of AKT signaling promotes cell growth and survival in alpha7beta1 integrin-mediated alleviation of muscular dystrophy. *Biochim Biophys Acta, 1812*(4), 439-446. doi: 10.1016/j.bbadis.2011.01.002

Britsch, S. (2007). The neuregulin-I/ErbB signaling system in development and disease. *Adv Anat Embryol Cell Biol, 190*, 1-65.

Bulfield, G., Siller, W. G., Wight, P. A., & Moore, K. J. (1984). X chromosome-linked muscular dystrophy (mdx) in the mouse. *Proc Natl Acad Sci U S A, 81*(4), 1189-1192.

Bushby, K., Finkel, R., Birnkrant, D. J., Case, L. E., Clemens, P. R., Cripe, L., . . . Constantin, C. (2010). Diagnosis and management of Duchenne muscular dystrophy, part 1: diagnosis, and pharmacological and psychosocial management. *Lancet Neurol, 9*(1), 77-93. doi: 10.1016/s1474-4422(09)70271-6

Chamberlain, J. S., Metzger, J., Reyes, M., Townsend, D., & Faulkner, J. A. (2007). Dystrophin-deficient mdx mice display a reduced life span and are susceptible to spontaneous rhabdomyosarcoma. *Faseb j, 21*(9), 2195-2204. doi: 10.1096/fj.06-7353com

Corfas, G., Velardez, M. O., Ko, C. P., Ratner, N., & Peles, E. (2004). Mechanisms and roles of axon-Schwann cell interactions. *J Neurosci, 24*(42), 9250-9260. doi: 10.1523/jneurosci.3649-04.2004

Cros, D., Harnden, P., Pellissier, J. F., & Serratrice, G. (1989). Muscle hypertrophy in Duchenne muscular dystrophy. A pathological and morphometric study. *J Neurol, 236*(1), 43-47.

Cyrulnik, S. E., Fee, R. J., Batchelder, A., Kiefel, J., Goldstein, E., & Hinton, V. J. (2008). Cognitive and adaptive deficits in young children with Duchenne muscular dystrophy (DMD). *J Int Neuropsychol Soc, 14*(5), 853-861. doi: 10.1017/s135561770808106x

Cyrulnik, S. E., Fee, R. J., De Vivo, D. C., Goldstein, E., & Hinton, V. J. (2007). Delayed developmental language milestones in children with Duchenne's muscular dystrophy. *J Pediatr, 150*(5), 474-478. doi: 10.1016/j.jpeds.2006.12.045

Davies, K. E., & Nowak, K. J. (2006). Molecular mechanisms of muscular dystrophies: old and new players. *Nat Rev Mol Cell Biol, 7*(10), 762-773. doi: 10.1038/nrm2024

Davies, K. E., Pearson, P. L., Harper, P. S., Murray, J. M., O'Brien, T., Sarfarazi, M., & Williamson, R. (1983). Linkage analysis of two cloned DNA sequences flanking the Duchenne muscular dystrophy locus on the short arm of the human X chromosome. *Nucleic Acids Res, 11*(8), 2303-2312.

Earp, H. S., 3rd, Calvo, B. F., & Sartor, C. I. (2003). The EGF receptor family--multiple roles in proliferation, differentiation, and neoplasia with an emphasis on HER4. *Trans Am Clin Climatol Assoc, 114*, 315-333; discussion 333-314.

Emery, A. E., & Emery, M. L. (1993). Edward Meryon (1809-1880) and muscular dystrophy. *J Med Genet, 30*(6), 506-511.

Fagerlund, M. J., & Eriksson, L. I. (2009). Current concepts in neuromuscular transmission. *Br J Anaesth, 103*(1), 108-114. doi: 10.1093/bja/aep150

Falls, D. L. (2003). Neuregulins: functions, forms, and signaling strategies. *Exp Cell Res, 284*(1), 14-30.

Fang, S. J., Wu, X. S., Han, Z. H., Zhang, X. X., Wang, C. M., Li, X. Y., . . . Zhang, J. L. (2010). Neuregulin-1 preconditioning protects the heart against ischemia/reperfusion injury through a PI3K/Akt-dependent mechanism. *Chin Med J (Engl), 123*(24), 3597-3604.

Ferlini, A., Neri, M., & Gualandi, F. (2013). The medical genetics of dystrophinopathies: molecular genetic diagnosis and its impact on clinical practice. *Neuromuscul Disord, 23*(1), 4-14. doi: 10.1016/j.nmd.2012.09.002

Ferraro, E., Molinari, F., & Berghella, L. (2012). Molecular control of neuromuscular junction development. *J Cachexia Sarcopenia Muscle, 3*(1), 13-23. doi: 10.1007/s13539-011-0041-7

Finder, J. D., Birnkrant, D., Carl, J., Farber, H. J., Gozal, D., Iannaccone, S. T., . . . Sterni, L. (2004). Respiratory care of the patient with Duchenne muscular dystrophy: ATS consensus statement. *Am J Respir Crit Care Med, 170*(4), 456-465. doi: 10.1164/rccm.200307-885ST

Fromm, L., & Burden, S. J. (2001). Neuregulin-1-stimulated phosphorylation of GABP in skeletal muscle cells. *Biochemistry, 40*(17), 5306-5312.

Gramolini, A. O., Angus, L. M., Schaeffer, L., Burton, E. A., Tinsley, J. M., Davies, K. E., . . . Jasmin, B. J. (1999). Induction of utrophin gene expression by heregulin in skeletal muscle cells: role of the N-box motif and GA binding protein. *Proc Natl Acad Sci U S A, 96*(6), 3223-3227.

Han, R., Rader, E. P., Levy, J. R., Bansal, D., & Campbell, K. P. (2011). Dystrophin deficiency exacerbates skeletal muscle pathology in dysferlin-null mice. *Skelet Muscle, 1*(1), 35. doi: 10.1186/2044-5040-1-35

Handschin, C., Kobayashi, Y. M., Chin, S., Seale, P., Campbell, K. P., & Spiegelman, B. M. (2007). PGC-1alpha regulates the neuromuscular junction program and ameliorates Duchenne muscular dystrophy. *Genes Dev, 21*(7), 770-783. doi: 10.1101/gad.1525107

Head, S. I. (1993). Membrane potential, resting calcium and calcium transients in isolated muscle fibres from normal and dystrophic mice. *J Physiol, 469*, 11-19.

Heydemann, A., & McNally, E. M. (2004). Regenerating more than muscle in muscular dystrophy. *Circulation, 110*(21), 3290-3292. doi: 10.1161/01.cir.0000149847.84152.0b

Hoffman, E. P., Brown, R. H., Jr., & Kunkel, L. M. (1987). Dystrophin: the protein product of the Duchenne muscular dystrophy locus. *Cell, 51*(6), 919-928.

Holmes, W. E., Sliwkowski, M. X., Akita, R. W., Henzel, W. J., Lee, J., Park, J. W., . . . et al. (1992). Identification of heregulin, a specific activator of p185erbB2. *Science, 256*(5060), 1205-1210.

Im, W. B., Phelps, S. F., Copen, E. H., Adams, E. G., Slightom, J. L., & Chamberlain, J. S. (1996). Differential expression of dystrophin isoforms in strains of mdx mice with different mutations. *Hum Mol Genet, 5*(8), 1149-1153.

Imbert, N., Cognard, C., Duport, G., Guillou, C., & Raymond, G. (1995). Abnormal calcium homeostasis in Duchenne muscular dystrophy myotubes contracting in vitro. *Cell Calcium, 18*(3), 177-186.

Jaworski, A., & Burden, S. J. (2006). Neuromuscular synapse formation in mice lacking motor neuron- and skeletal muscle-derived Neuregulin-1. *J Neurosci, 26*(2), 655-661. doi: 10.1523/jneurosci.4506-05.2006

Jejurikar, S. S., & Kuzon, W. M., Jr. (2003). Satellite cell depletion in degenerative skeletal muscle. *Apoptosis, 8*(6), 573-578. doi: 10.1023/a:1026127307457

Joshi, N., & Rajeshwari, K. (2009). Deflazacort. *J Postgrad Med, 55*(4), 296-300. doi: 10.4103/0022-3859.58942

Khurana, T. S., & Davies, K. E. (2003). Pharmacological strategies for muscular dystrophy. *Nat Rev Drug Discov, 2*(5), 379-390. doi: 10.1038/nrd1085

Kong, J., & Anderson, J. E. (1999). Dystrophin is required for organizing large acetylcholine receptor aggregates. *Brain Res, 839*(2), 298-304.

Krag, T. O., Bogdanovich, S., Jensen, C. J., Fischer, M. D., Hansen-Schwartz, J., Javazon, E. H., . . . Khurana, T. S. (2004). Heregulin ameliorates the dystrophic phenotype in mdx mice. *Proc Natl Acad Sci U S A, 101*(38), 13856-13860. doi: 10.1073/pnas.0405972101

Mallouk, N., Jacquemond, V., & Allard, B. (2000). Elevated subsarcolemmal Ca2+ in mdx mouse skeletal muscle fibers detected with Ca2+-activated K+ channels. *Proc Natl Acad Sci U S A, 97*(9), 4950-4955.

Manzur, A. Y., Kuntzer, T., Pike, M., & Swan, A. (2004). Glucocorticoid corticosteroids for Duchenne muscular dystrophy. *Cochrane Database Syst Rev*(2), Cd003725. doi: 10.1002/14651858.CD003725.pub2

Marques, M. J., Pertille, A., Carvalho, C. L., & Santo Neto, H. (2007). Acetylcholine receptor organization at the dystrophic extraocular muscle neuromuscular junction. *Anat Rec (Hoboken), 290*(7), 846-854. doi: 10.1002/ar.20525

Marshall, J. L., & Crosbie-Watson, R. H. (2013). Sarcospan: a small protein with large potential for Duchenne muscular dystrophy. *Skelet Muscle, 3*(1), 1. doi: 10.1186/2044-5040-3-1

Matthew K. Ball, D. H. C., Kelly Ezell, Jessica B. Henley, Paul R. Standley, Wade A. Grow. (2013). Antibody to MyoD or Myogenin Decreases Acetylcholine Receptor Clustering in C2C12 Myotube Culture. *CellBio, 2*(3).

McMahon, D. K., Anderson, P. A., Nassar, R., Bunting, J. B., Saba, Z., Oakeley, A. E., & Malouf, N. N. (1994). C2C12 cells: biophysical, biochemical, and immunocytochemical properties. *Am J Physiol, 266*(6 Pt 1), C1795-1802.

Mendell, J. R., & Lloyd-Puryear, M. (2013). Report of MDA muscle disease symposium on newborn screening for Duchenne muscular dystrophy. *Muscle Nerve, 48*(1), 21-26. doi: 10.1002/mus.23810

Mercuri, E., & Muntoni, F. (2013). Muscular dystrophies. *Lancet, 381*(9869), 845-860. doi: 10.1016/s0140-6736(12)61897-2

Mourkioti, F., Kustan, J., Kraft, P., Day, J. W., Zhao, M. M., Kost-Alimova, M., . . . Blau, H. M. (2013). Role of telomere dysfunction in cardiac failure in Duchenne muscular dystrophy. *Nat Cell Biol, 15*(8), 895-904. doi: 10.1038/ncb2790

Nagaraju, K., & Willmann, R. (2009). Developing standard procedures for murine and canine efficacy studies of DMD therapeutics: report of two expert workshops on "Pre-clinical testing for Duchenne dystrophy": Washington DC, October 27th–28th 2007 and Zürich, June 30th-July 1st 2008. *Neuromuscular Disorders, 19*(7), 502-506. doi: http://dx.doi.org/10.1016/j.nmd.2009.05.003

Negro, A., Brar, B. K., & Lee, K. F. (2004). Essential roles of Her2/erbB2 in cardiac development and function. *Recent Prog Horm Res, 59*, 1-12.

Newbern, J., & Birchmeier, C. (2010). Nrg1/ErbB signaling networks in Schwann cell development and myelination. *Semin Cell Dev Biol, 21*(9), 922-928. doi: 10.1016/j.semcdb.2010.08.008

Nowak, K. J., & Davies, K. E. (2004). Duchenne muscular dystrophy and dystrophin: pathogenesis and opportunities for treatment. *EMBO Rep, 5*(9), 872-876. doi: 10.1038/sj.embor.7400221

Odiete, O., Hill, M. F., & Sawyer, D. B. (2012). Neuregulin in cardiovascular development and disease. *Circ Res, 111*(10), 1376-1385. doi: 10.1161/circresaha.112.267286

Ohlendiec, K. G. C. a. K. (2002). Abnormal Calcium Handling in Muscular Dystrophy *Kevin G Culligan and Kay Ohlendiec, 12*(4), 147-157.

Pane, M., Lombardo, M. E., Alfieri, P., D'Amico, A., Bianco, F., Vasco, G., . . . Mercuri, E. (2012). Attention deficit hyperactivity disorder and cognitive function in Duchenne muscular dystrophy: phenotype-genotype correlation. *J Pediatr, 161*(4), 705-709.e701. doi: 10.1016/j.jpeds.2012.03.020

Parent, A. (2005). Duchenne De Boulogne: a pioneer in neurology and medical photography. *Can J Neurol Sci, 32*(3), 369-377.

Passamano, L., Taglia, A., Palladino, A., Viggiano, E., D'Ambrosio, P., Scutifero, M., . . . Politano, L. (2012). Improvement of survival in Duchenne Muscular Dystrophy: retrospective analysis of 835 patients. *Acta Myol, 31*(2), 121-125.

Pato, C. N., Davis, M. H., Doughty, M. J., Bryant, S. H., & Gruenstein, E. (1983). Increased membrane permeability to chloride in Duchenne muscular dystrophy fibroblasts and its relationship to muscle function. *Proc Natl Acad Sci U S A, 80*(15), 4732-4736.

Personius, K. E., & Sawyer, R. P. (2005). Terminal Schwann cell structure is altered in diaphragm of mdx mice. *Muscle Nerve, 32*(5), 656-663. doi: 10.1002/mus.20405

Plowman, G. D., Green, J. M., Culouscou, J. M., Carlton, G. W., Rothwell, V. M., & Buckley, S. (1993). Heregulin induces tyrosine phosphorylation of HER4/p180erbB4. *Nature, 366*(6454), 473-475. doi: 10.1038/366473a0

Pons, F., Robert, A., Marini, J. F., & Leger, J. J. (1994). Does utrophin expression in muscles of mdx mice during postnatal development functionally compensate for dystrophin deficiency? *J Neurol Sci, 122*(2), 162-170.

Pratt, S. J., Shah, S. B., Ward, C. W., Inacio, M. P., Stains, J. P., & Lovering, R. M. (2013). Effects of in vivo injury on the neuromuscular junction in healthy and dystrophic muscles. *J Physiol, 591*(Pt 2), 559-570. doi: 10.1113/jphysiol.2012.241679

Roberts, R. G. (1995). Dystrophin, its gene, and the dystrophinopathies. *Adv Genet, 33*, 177-231.

Roskoski, R., Jr. (2012). ERK1/2 MAP kinases: structure, function, and regulation. *Pharmacol Res, 66*(2), 105-143. doi: 10.1016/j.phrs.2012.04.005

Ryder-Cook, A. S., Sicinski, P., Thomas, K., Davies, K. E., Worton, R. G., Barnard, E. A., . . . Barnard, P. J. (1988). Localization of the mdx mutation within the mouse dystrophin gene. *Embo j, 7*(10), 3017-3021.

Sacco, A., Mourkioti, F., Tran, R., Choi, J., Llewellyn, M., Kraft, P., . . . Blau, H. M. (2010). Short telomeres and stem cell exhaustion model Duchenne muscular dystrophy in mdx/mTR mice. *Cell, 143*(7), 1059-1071. doi: 10.1016/j.cell.2010.11.039

Saito, K., Ikeya, K., Kondo, E., Yamauchi, A., Komine, S., & Fukuyama, Y. (1993). [Molecular genetics of Duchenne/Becker muscular dystrophy]. *Nihon Rinsho, 51*(9), 2420-2427.

Sakamoto, K., & Goodyear, L. J. (2002). Invited review: intracellular signaling in contracting skeletal muscle. *J Appl Physiol (1985), 93*(1), 369-383. doi: 10.1152/japplphysiol.00167.2002

Sander, M., Chavoshan, B., Harris, S. A., Iannaccone, S. T., Stull, J. T., Thomas, G. D., & Victor, R. G. (2000). Functional muscle ischemia in neuronal nitric oxide synthase-deficient skeletal muscle of children with Duchenne muscular dystrophy. *Proc Natl Acad Sci U S A, 97*(25), 13818-13823. doi: 10.1073/pnas.250379497

Schara, U., Mortier, & Mortier, W. (2001). Long-Term Steroid Therapy in Duchenne Muscular Dystrophy-Positive Results versus Side Effects. *J Clin Neuromuscul Dis, 2*(4), 179-183.

Schertzer, J. D., van der Poel, C., Shavlakadze, T., Grounds, M. D., & Lynch, G. S. (2008). Muscle-specific overexpression of IGF-I improves E-C coupling in skeletal muscle fibers from dystrophic mdx mice. *Am J Physiol Cell Physiol, 294*(1), C161-168. doi: 10.1152/ajpcell.00399.2007

Schiaffino, S., & Mammucari, C. (2011). Regulation of skeletal muscle growth by the IGF1-Akt/PKB pathway: insights from genetic models. *Skelet Muscle, 1*(1), 4. doi: 10.1186/2044-5040-1-4

Sharma, K. R., Mynhier, M. A., & Miller, R. G. (1995). Muscular fatigue in Duchenne muscular dystrophy. *Neurology, 45*(2), 306-310.

Shiao, T., Fond, A., Deng, B., Wehling-Henricks, M., Adams, M. E., Froehner, S. C., & Tidball, J. G. (2004). Defects in neuromuscular junction structure in dystrophic muscle are corrected by expression of a NOS transgene in dystrophin-deficient muscles, but not in muscles lacking alpha- and beta1-syntrophins. *Hum Mol Genet, 13*(17), 1873-1884. doi: 10.1093/hmg/ddh204

Stassart, R. M., Fledrich, R., Velanac, V., Brinkmann, B. G., Schwab, M. H., Meijer, D., . . . Nave, K. A. (2013). A role for Schwann cell-derived neuregulin-1 in remyelination. *Nat Neurosci, 16*(1), 48-54. doi: 10.1038/nn.3281

Sudhof, T. C. (2004). The synaptic vesicle cycle. *Annu Rev Neurosci, 27*, 509-547. doi: 10.1146/annurev.neuro.26.041002.131412

Sugiyama, J. E., Glass, D. J., Yancopoulos, G. D., & Hall, Z. W. (1997). Laminin-induced acetylcholine receptor clustering: an alternative pathway. *J Cell Biol, 139*(1), 181-191.

Tansey, M. G., Chu, G. C., & Merlie, J. P. (1996). ARIA/HRG regulates AChR epsilon subunit gene expression at the neuromuscular synapse via activation of phosphatidylinositol 3-kinase and Ras/MAPK pathway. *J Cell Biol, 134*(2), 465-476.

Tayeb, M. T. (2010). Deletion mutations in Duchenne muscular dystrophy (DMD) in Western Saudi children. *Saudi J Biol Sci, 17*(3), 237-240. doi: 10.1016/j.sjbs.2010.04.008

Tinsley, J., Deconinck, N., Fisher, R., Kahn, D., Phelps, S., Gillis, J. M., & Davies, K. (1998). Expression of full-length utrophin prevents muscular dystrophy in mdx mice. *Nat Med, 4*(12), 1441-1444. doi: 10.1038/4033

Tinsley, J. M., Blake, D. J., Zuellig, R. A., & Davies, K. E. (1994). Increasing complexity of the dystrophin-associated protein complex. *Proc Natl Acad Sci U S A, 91*(18), 8307-8313.

Trinidad, J. C., & Cohen, J. B. (2004). Neuregulin inhibits acetylcholine receptor aggregation in myotubes. *J Biol Chem, 279*(30), 31622-31628. doi: 10.1074/jbc.M400044200

Turner, P. R., Westwood, T., Regen, C. M., & Steinhardt, R. A. (1988). Increased protein degradation results from elevated free calcium levels found in muscle from mdx mice. *Nature, 335*(6192), 735-738. doi: 10.1038/335735a0

Ueda, H., Oikawa, A., Nakamura, A., Terasawa, F., Kawagishi, K., & Moriizumi, T. (2005). Neuregulin receptor ErbB2 localization at T-tubule in cardiac and skeletal muscle. *J Histochem Cytochem, 53*(1), 87-91. doi: 10.1369/jhc.4A6341.2005

Vartanian, T., Fischbach, G., & Miller, R. (1999). Failure of spinal cord oligodendrocyte development in mice lacking neuregulin. *Proc Natl Acad Sci U S A, 96*(2), 731-735.

Verma, S., Anziska, Y., & Cracco, J. (2010). Review of Duchenne muscular dystrophy (DMD) for the pediatricians in the community. *Clin Pediatr (Phila), 49*(11), 1011-1017. doi: 10.1177/0009922810378738

Voisin, V., & de la Porte, S. (2004). Therapeutic strategies for Duchenne and Becker dystrophies. *Int Rev Cytol, 240*, 1-30. doi: 10.1016/s0074-7696(04)40001-1

Wallace, G. Q., & McNally, E. M. (2009). Mechanisms of muscle degeneration, regeneration, and repair in the muscular dystrophies. *Annu Rev Physiol, 71*, 37-57. doi: 10.1146/annurev.physiol.010908.163216

Weir, A. P., Morgan, J. E., & Davies, K. E. (2004). A-utrophin up-regulation in mdx skeletal muscle is independent of regeneration. *Neuromuscul Disord, 14*(1), 19-23.

Wells, D. J. (2008). Treatments for muscular dystrophy: increased treatment options for Duchenne and related muscular dystropies. *Gene Ther, 15*(15), 1077-1078. doi: 10.1038/gt.2008.97

Wojtaszewski, J. F., Nielsen, P., Kiens, B., & Richter, E. A. (2001). Regulation of glycogen synthase kinase-3 in human skeletal muscle: effects of food intake and bicycle exercise. *Diabetes, 50*(2), 265-269.

Zhao, Y. Y., Sawyer, D. R., Baliga, R. R., Opel, D. J., Han, X., Marchionni, M. A., & Kelly, R. A. (1998). Neuregulins promote survival and growth of cardiac myocytes. Persistence of ErbB2 and ErbB4 expression in neonatal and adult ventricular myocytes. *J Biol Chem, 273*(17), 10261-10269.